Spectroscopic Investigation of the Formation and Disruption of Hydrogen Bonds in Pharmaceutical Semicrystalline Dispersions

Peer-reviewed author version

Duong, Tu Van; REEKMANS, Gunter; Venkatesham, Akkaladevi; Van Aerschot, Arthur; ADRIAENSENS, Peter; Van Humbeeck, Jan & Van den Mooter, Guy (2017) Spectroscopic Investigation of the Formation and Disruption of Hydrogen Bonds in Pharmaceutical Semicrystalline Dispersions. In: MOLECULAR PHARMACEUTICS, 14(5), p. 1726-1741.

DOI: 10.1021/acs.molpharmaceut.6b01172
Handle: http://hdl.handle.net/1942/24218

Spectroscopic investigation of the formation and disruption of hydrogen bonds in pharmaceutical semi-crystalline dispersions

Tu Van Duong,[†,⊥] Gunter Reekmans,[§] Akkaladevi Venkatesham,[‡] Arthur Van Aerschot,[‡] Peter Adriaensens,[§] Jan Van Humbeeck,[¶] and Guy Van den Mooter[,†]*

[†] Drug Delivery and Disposition, Department of Pharmaceutical and Pharmacological Sciences, KU Leuven, Campus Gasthuisberg O&N2, Herestraat 49 b921, 3000 Leuven, Belgium

[⊥] Department of Pharmaceutics, Hanoi University of Pharmacy, 13-15 Le Thanh Tong, Hoan Kiem, Ha Noi, Vietnam

[§] Applied and Analytical Chemistry, Institute for Materials Research, Hasselt University, Diepenbeek BE-3590, Belgium

[‡] Medicinal Chemistry, Rega Institute for Medical Research, KU Leuven, Herestraat 49 b1041, 3000 Leuven, Belgium

[¶] Department of Materials Engineering, KU Leuven, Campus Arenberg, Kasteelpark Arenberg 44 b2450, 3001 Heverlee, Belgium

KEYWORDS

solid dispersions, indomethacin, polyethylene glycol, amorphous, crystallization, hydrogen bonding, modulated differential scanning calorimetry, X-ray diffraction, Fourier transform infrared spectroscopy, nuclear magnetic resonance spectroscopy

Table of Contents Graphic

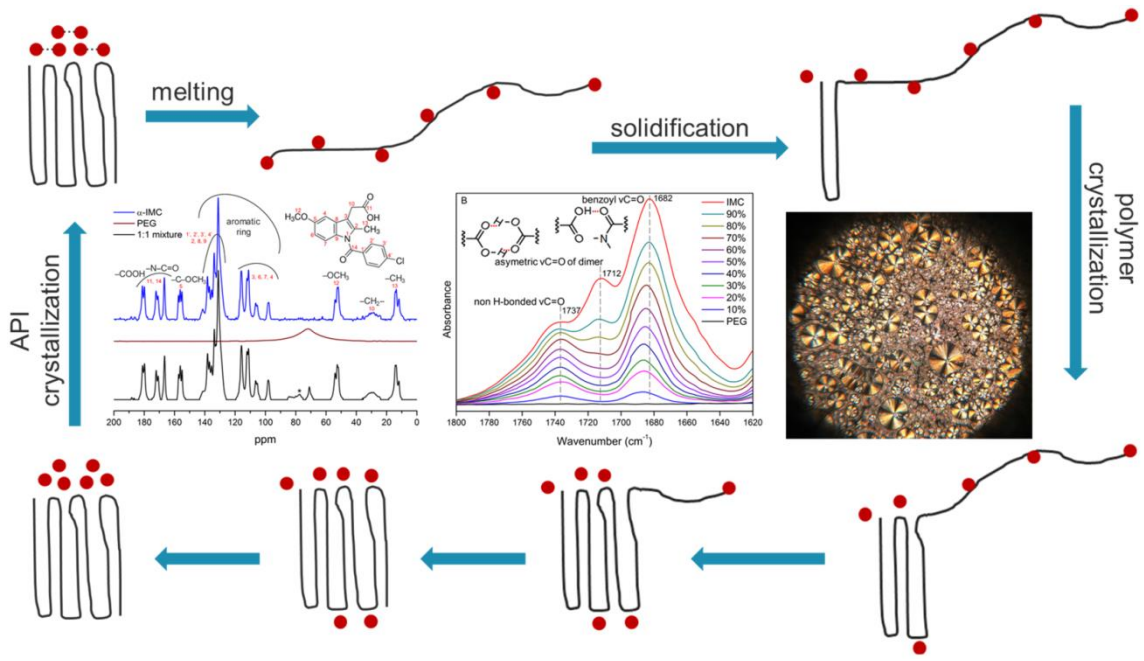

ABSTRACT

We recently found that indomethacin (IMC) can effectively act as a powerful crystallization inhibitor for polyethylene glycol 6000 (PEG) despite the fact that the absence of interactions between the drug and the carrier in the solid state was reported in the literature. However, in the present study, we investigate the possibility of drug-carrier interactions in the liquid state to explain the polymer crystallization inhibition effect of IMC. We also aim to discover other potential PEG crystallization inhibitors. Drug-carrier interactions in both liquid and solid state are characterized by variable temperature Fourier transform infrared spectroscopy (FTIR) and cross-polarization magic angle spinning ^{13}C nuclear magnetic resonance spectroscopy (CP/MAS NMR). In the liquid state, FTIR data show evidence of the breaking of hydrogen bonding between IMC molecules to form interactions of the IMC monomer with PEG. The drug-carrier interactions are disrupted upon storage and polymer crystallization, resulting in segregation of IMC from PEG crystals that can be observed under polarized light microscopy. This process is further confirmed by ^{13}C NMR since in the liquid state, when the IMC:PEG monomer units ratio is below 2:1, IMC signals are undetectable because of the loss of cross-

polarization efficiency in the mobile IMC molecules upon attachment to PEG chains via hydrogen bonding. This suggests that each ether oxygen of the PEG unit can form hydrogen bonds with two IMC molecules. The NMR spectrum of IMC shows no change in solid dispersions with PEG upon storage, indicating the absence of interactions in the solid state, hence confirming previous studies. The drug-carrier interactions in the liquid state elucidate the crystallization inhibition effect of IMC on PEG as well as other semi-crystalline polymers such as poloxamer and Gelucire®. However, hydrogen bonding is a necessary but apparently not a sufficient condition for the polymer crystallization inhibition. Screening of crystallization inhibitors of semi-crystalline polymers discovers numerous candidates that exhibit the same behavior as IMC, demonstrating a general pattern of polymer crystallization inhibition rather than a particular case. Furthermore, the crystallization inhibition effect of drugs on PEG is independent on the carrier molecular weight. These mechanistic findings on the formation and disruption of hydrogen bonds in semi-crystalline dispersions can be extended to amorphous dispersions and are of significant importance for preparation of solid dispersions with consistent and reproducible physicochemical properties.

INTRODUCTION

Despite being considered as one of the most powerful strategies to overcome the limited solubility and dissolution rate of poorly water soluble active pharmaceutical ingredients (APIs) which account for approximately 40% of marketed drugs and most current drug development candidates,[1] the application of solid dispersions has been largely restricted by physical stability problems leading to bioavailability variation.[2, 3] This emphasizes the need of further mechanistic understanding of solid dispersions at the molecular level in order to improve product qualities.

In a system containing API and carrier, the properties of each component as well as their mutual interactions cooperatively dictate the performance of solid dispersions. In fact, as the carrier normally constitutes the largest part of the formulation, its characteristics will greatly contribute to the properties and behavior of solid dispersions.[4, 5] However, studies on solid dispersions have mainly focused on how carriers affect properties of APIs. There have been only few studies dealing with the influence of APIs and preparation processes on the properties of carriers as well as the behavior of the carriers in the system.

For amorphous carriers, although the amorphous state of the carriers remain unchanged in either the absence or presence of APIs, the modifications in their conformation under the influence of solvent quality,[6] pH,[7, 8] ionic strength[9] or mechanical stress[10] might result in significant differences in drug-carrier interactions, the drug stabilization and supersaturation maintenance effect of the carriers.[5] The story becomes even more complicated with semi-crystalline carriers like polyethylene glycol. On the one hand, the presence of PEG either accelerated, slowed down or had no influence on the crystallization process of APIs; on the other hand, APIs have been found to affect the crystallization of the polymer[11, 12] that in turn might influence the microstructure and hence the physicochemical properties and the pharmaceutical performance of the system.[4] Therefore, thorough understanding of the behavior of both APIs and carriers

will be of great importance for preparation of solid dispersions with consistent and reproducible performance.

In a recent paper, we reported that indomethacin acted as an effective crystallization inhibitor of PEG[13] and at certain drug loading, the drug was able to maintain the amorphous state of PEG for months or even years. Increasing the drug content results in higher stability and slows down the crystallization rate of the amorphous polymer. In addition, depending on the interplay between the crystallization rate of PEG and the diffusion rate of indomethacin upon changing the drug loading, the crystallization of the polymer may give rise to a single amorphous phase or generate amorphous–amorphous phase separation, producing a polymer-rich domain and a drug-rich domain which exhibits two distinct glass transition temperatures (T_gs). These observations demonstrate a wide range in physicochemical properties of PEG-IMC dispersions as a result of the complex nature in crystallization of the system, which should be taken into account during preparation and storage.

IMC is indeed not the only API that impedes the crystallization of PEG but it is, to the best of our knowledge, the first low molecular weight drug that can retain amorphous PEG for such long periods. Other APIs including chlorpropamide, aceclofenac,[11] ibuprofen, benzocaine,[12] temazepam[14] could also decrease the growth rate of PEG crystals, yet the polymer still crystallized extremely fast within few minutes. The first idea that comes to mind as an explanation for the inhibition effect of IMC on the PEG crystallization would be specific drug-carrier interactions. However, all studies involving PEG-IMC solid dispersions consistently reported the absence of any interactions.[15-17] Another research question is whether other PEG crystallization inhibitors do exist, or is this an exclusive characteristic of IMC? Therefore, the present work aims to elucidate the origin of the inhibition effect of IMC on the PEG crystallization, and to discover other potential PEG crystallization inhibitors.

EXPERIMENTAL SECTION

Materials

The main model API, γ-IMC (melting point – T_m: 161°C, T_g: 45°C), was purchased from Fagron (Saint-Denis, France). The α polymorph of IMC was prepared by the method described by Kaneniwa et al.,[18] starting with dissolving an excessive amount of γ-IMC in ethanol at 80°C. The undissolved drug was filtered off then deionized water was added to the saturated ethanol solution of IMC. The precipitated crystals were obtained by filtration and dried in a phosphorous pentoxide containing desiccator under vacuum at room temperature. Amorphous IMC was generated by melting γ-IMC at 165°C in 3 minutes, followed by quench cooling in liquid nitrogen. The material was then stored over phosphorous pentoxide at -25°C.

Other APIs including suprofen (T_m: 124°C, T_g: 8°C), indoprofen (T_m: 212°C, T_g: 50°C), fenoprofen (T_m: 170°C, T_g: 36°C) and fenofiobrate (T_m: 81°C, T_g: -19°C) were obtained from Sigma-Aldrich (St. Louis, MO, USA). Flurbiprofen (T_m: 115°C, Tg: -6°C) was purchased from Acros Organics N.V. (Geel, Belgium). Ketoprofen (T_m: 95°C, T_g: -3°C) was supplied by Tokyo Chemical Industry Co. (Tokyo, Japan). Ibuprofen (T_m: 77°C, T_g: -45°C) and tiaprofenic acid (T_m: 96°C, T_g: -6°C) were purchased from Certa N.V. (Braine-l'Alleud, Belgium) and Roussel Uclaf S.A. (Romainville, France), respectively.

PEG 6000 (T_m: 60°C) was obtained from Sigma-Aldrich (Geel, Belgium) while PEG 100,000 (T_m: 66°C) and PEG 8,000,000 (T_m: 66°C) were purchased from Sigma-Aldrich in Steinheim, Germany. PEG 4000 (T_m: 60°C) and PEG 20,000 (T_m: 65°C) were supplied by Fagron N.V. (Waregem, Belgium) and Merck KGaA (Darmstadt, Germany), respectively.

The other semi-crystalline polymers namely poloxamer 188 (Lutrol F68, T_m: 54°C), poloxamer 338 (Lutrol F108, T_m: 59°C) and poloxamer 407 (Lutrol F127, T_m: 57°C) were all purchased from BASF (Ludwigshafen, Germany). Gelucire 50/13 (T_m: 50°C) and Gelucire 44/144 (T_m:

44ºC) were obtained from Gattefossé (Saint-Priest, France). All chemicals were of reagent grade or better and were used as received without further purification.

Sample Preparation

PEG-APIs dispersions were prepared by heating the mixture of the two components to *ca*. 5°C above the melting points of the APIs under stirring and keeping the samples at this temperature for 3 minutes to ensure complete melting, followed by solidification of the melt. The samples were stored at room temperature in a desiccator containing phosphorus pentoxide.

Modulated Differential Scanning Calorimetry (m-DSC)

Thermal properties of dispersions were analyzed on a Q2000 m-DSC (TA instruments, Leatherhead, UK), equipped with a refrigerated cooling system RCS90 under inert dry nitrogen purge at a flow rate of 50 ml/min. Indium and n-octadecane were used for temperature calibration. Melting enthalpy and heat capacity were calibrated using indium and sapphire disks, respectively.

The samples were crimped in aluminium pans then kept isothermal at *ca*. 5°C above the melting temperatures of APIs during 3 minutes before cooling to -75°C at a cooling rate of 20°C/min. Afterwards, the samples were subjected to heating from -75°C to *ca*. 5°C above the melting points of the APIs using an underlying heating rate of 5°C/min with a modulation amplitude and period of ±0.636 °C and 40 s, respectively. All samples were analyzed in duplicate. DSC thermograms were acquired using Thermal Advantage software and analyzed by Universal Analysis software (version 4.4, TA Instruments).

X-ray Diffraction (XRD)

Diffraction patterns of samples were measured in transmission mode between $4° \leq 2\theta \leq 40°$ with 0.0167° step size and 200 s counting time per step using an automated X'pert PRO diffractometer (PANalytical, Almelo, The Netherlands) with a Cu tube (Kα $\lambda = 1.5418$ Å). The

generator was set at 45 kV and 40 mA. The X'pert Data Collector was used for data acquisition, and data analysis was performed using the X'Pert Data Viewer and X'Pert HighScore Plus (PANalytical, Almelo, The Netherlands).

Fourier Transform Infrared Spectroscopy

FTIR spectra were recorded on a Bruker Tensor II spectrophotometer (Bruker Optics GmbH, Ettlingen, Germany) utilizing a Golden Gate single attenuated total reflectance (ATR) accessory equipped with a temperature controller (Specac Ltd., Kent, UK) covering a wavenumber range from 400 to 4000 cm^{-1}. The final spectrum was the average of 64 scans accumulated using Bruker's Opus software 7.0, taken at 4 cm^{-1} resolution. The FTIR spectra of PEG-APIs dispersions were collected in both solid and liquid state at different temperatures.

^{13}C Nuclear Magnetic Resonance Spectroscopy

^{13}C CP/MAS NMR spectra were acquired using a Varian Unity Inova 400 spectrometer (Varian Inc., Palo Alto, USA) operating at a static magnetic field of 9.4 T. The aromatic signal of hexamethylbenzene was used to determine the Hartmann–Hahn condition for cross-polarization and to calibrate the carbon chemical shift scale (132.1 ppm). Magic angle spinning was performed at 5400 Hz, unless otherwise specified, making use of ceramic Si_3N_4 rotors. Potassium bromide was used to adjust the magic angle.

Other spectral parameters used were a 90° pulse length of 5.1 μs, a spectral width of 50 kHz, an acquisition time of 25 ms, a contact time for cross-polarization of 2 ms for IMC and dispersions and 0.125 ms for PEG, and a pulse delay of 7.5 s. High power proton decoupling was set to 65 kHz during the acquisition time. The proton spin–lattice (T_{1H}) relaxation times were measured via the chemical shift selective carbon nuclei by the inversion-recovery method. A preparation delay of five times the longest T_{1H} decay time was always respected.

The ^{13}C NMR spectra of PEG-APIs dispersions were collected in both solid and liquid state at different temperatures. Temperature was calibrated using lead nitrate. Samples were equilibrated at each temperature at least 10 minutes before data acquisition.

Polarized Light Microscopy (PLM)

Sample morphology and birefringence were investigated using an Olympus BX60 polarizing optical microscope (Olympus, Hamburg, Germany) equipped with a THMS600 hot stage and a TMS93 temperature controller (Linkam Scientific, Tadworth, UK). Samples were spread between two glass slides and kept at *ca*. 5°C above the melting points of APIs for 3 minutes on the hot stage before being cooled to room temperature at the cooling rate of 20°C/min. The presence of birefringence under polarized light was visualized and captured using a digital camera.

RESULTS

Screening of PEG Crystallization Inhibitors

A large screening of APIs was conducted to identify drugs that exhibit a similar behavior as IMC on PEG crystallization. Among these APIs, only 5 drugs namely ketoprofen, flurbiprofen, suprofen, tiaprofenic acid and fenoprofen can inhibit the crystallization of PEG during DSC measurements at drug loadings from at least 55%, 60%, 60%, 60% and 65%, respectively (Figure 1). As illustrated in the figure, at drug weight fractions below these minimum inhibition concentrations, melting peaks of PEG in the range from 35°C to 50°C and the preceding crystallization events were observed in the DSC thermograms. In contrast, when the drug loadings were above the critical values, no exothermic and endothermic events of PEG were detected, indicating the complete amorphous nature of the polymer. No crystallization signal of PEG was observed in all samples upon cooling (data not shown).

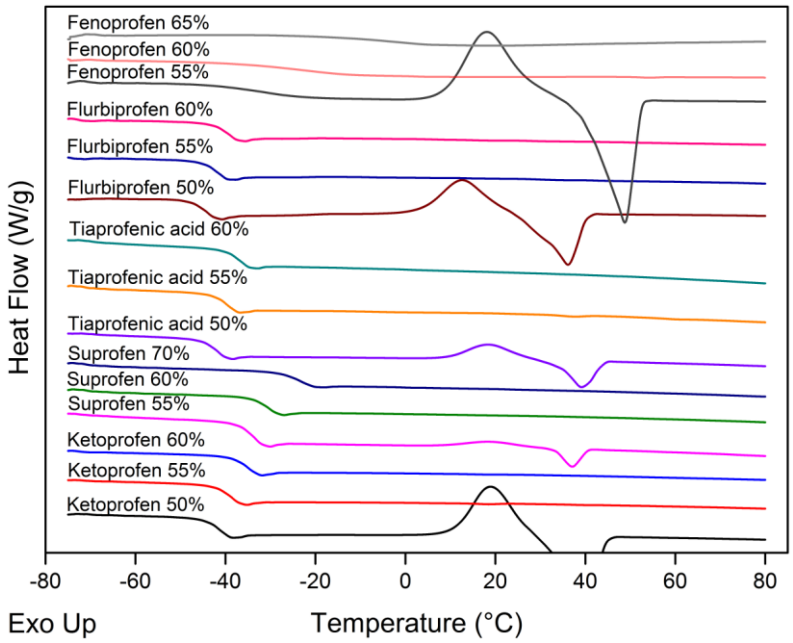

Figure 1. DSC thermograms with heat flow signal *vs*. temperature for samples containing different loadings of drugs in dispersions with PEG upon heating after being cooled from the melt.

In PEG-based dispersions, ketoprofen, suprofen, tiaprofenic acid and flurbiprofen exhibited time-dependent T_g shifting in a manner similar to that of IMC.[13] In this set of DSC experiments, PEG-APIs dispersions containing 50% drug loading were kept isothermal at *ca*. 5°C above the melting temperatures of the APIs during 3 minutes before cooling to 5°C at the cooling rate of 2°C/min. The samples were then stored at 5°C inside the DSC cell for predetermined time intervals and subsequently cooled to -75°C then directly heated to *ca*. 5°C above the melting points of the drug compounds at the heating rate of 5°C/min.

At the beginning, the dispersions showed only one T_g, representing a single homogeneous amorphous phase of the drug and the polymer (Figure 2). The evolution of a second T_g was noticed after a certain period as a result of PEG crystallization while amorphous drug remained intact, indicating amorphous-amorphous phase separation that forms a polymer-rich domain with lower and constant T_{g1}, and a drug-rich domain with higher and continuously increasing T_{g2} upon storage. The heat capacity jump at T_{g1} dramatically decreased due to the crystallization

of amorphous PEG before T_{g1} disappeared, demonstrating vanishing of the polymer-rich domain. The heat capacity jump at T_{g2} was rising as the ratio of drug/polymer in the drug-rich domain continued to increase until the decrease in amorphous polymer fraction in this region dominates the increase in amorphous drug, thus ultimately reducing the total size of the drug-rich domain.

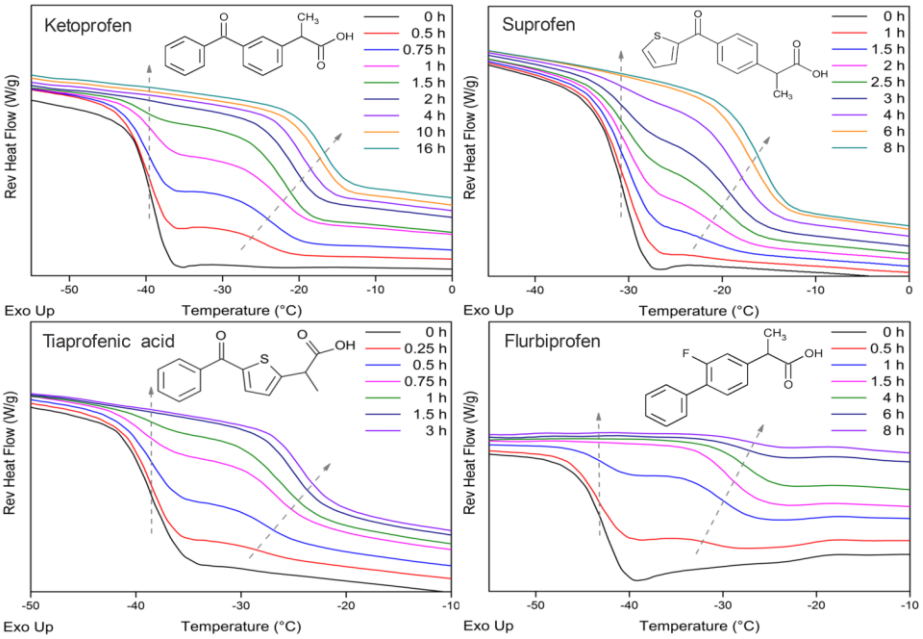

Figure 2. DSC thermograms with reversing heat flow signal *vs*. temperature for dispersions of 50% drug loading. Dispersions were stored inside the DSC cell for different time periods at 5°C.

The aforementioned data suggested that the crystallization inhibition of PEG is a general pattern of various drugs rather than a particular behavior of IMC. An interesting question is why these APIs inhibit the crystallization of PEG while many others do not. In our recent paper,[13] we argued that unelucidated factor(s) must play a role in the crystallization inhibition effect of IMC on PEG because no interaction between these two components was repeatedly reported in literature.[15-17] For ketoprofen, the absence of interactions with PEG was found by Margarit et al.[19] whereas Schachter et al. observed the opposite.[20] Flurbiprofen was able to form hydrogen bonding with PEG as reported by Ozeki et al[21] and Lacoulonche.[22, 23] No data on interaction

was available for dispersions of PEG with suprofen or tiaprofenic acid. The discrepancy in the drug-carrier interactions between PEG and these polymer crystallization inhibitors emphasizes the need for further elucidation.

The Role of Hydrogen Bonding in the Polymer Crystallization Inhibition

Due to the fact that all of these APIs contain a carboxylic acid functional group (Figure 2), hydrogen bonding is expected between the hydroxyl moiety of APIs and ether oxygen of PEG or between the end-standing hydroxyl groups of PEG and the acid carbonyl and/or benzoyl carbonyl of the APIs. As a matter of fact, the number of ether oxygens (135) present in PEG 6000 is much larger than the two hydroxyl end groups, thus the hydroxyl moiety of the drugs are more likely to donate a hydrogen in hydrogen bonding to the PEG ether acceptor group. In order to investigate the importance of drug-carrier interactions between IMC and PEG on the crystallization inhibition effect of the drug on the polymer, two derivatives of IMC with the carboxyl hydroxyl being substituted by an OCH_3 (ester) and NH_2 (amide) were synthesized. The synthetic procedures are provided in **Supporting information**, section S1.

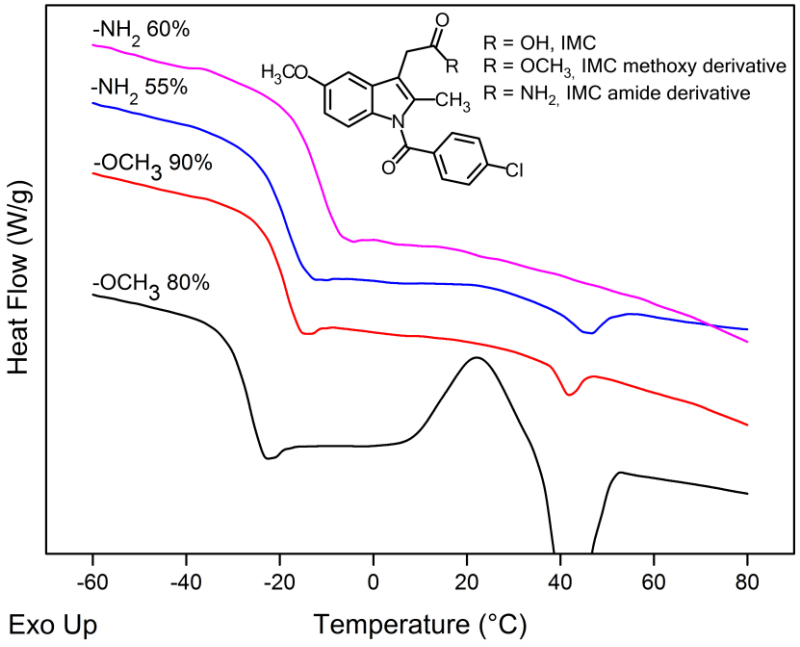

Figure 3. DSC thermograms with heat flow signal *vs*. temperature for dispersions of PEG and ester or amide derivative of IMC containing different loadings of the IMC derivatives.

Figure 3 shows that when the hydroxyl moiety of IMC was substituted by the methoxy group, the new derivative was unable to inhibit the polymer crystallization any longer, even at an extremely high drug loading of 90%, as exhibited by the melting peaks of PEG at *ca*. 45°C. The amide derivative, in contrast, could still effectively maintain the amorphous state of PEG at as low as 60% drug concentration because the new compound was able to form hydrogen bonds with PEG by donating a hydrogen of the amide group to the ether oxygen of the polymer. Exactly the same phenomenon was observed for ketoprofen and its methoxy or amide derivative in dispersions with PEG (see **Supporting information**, Section S2 and Figure S1).

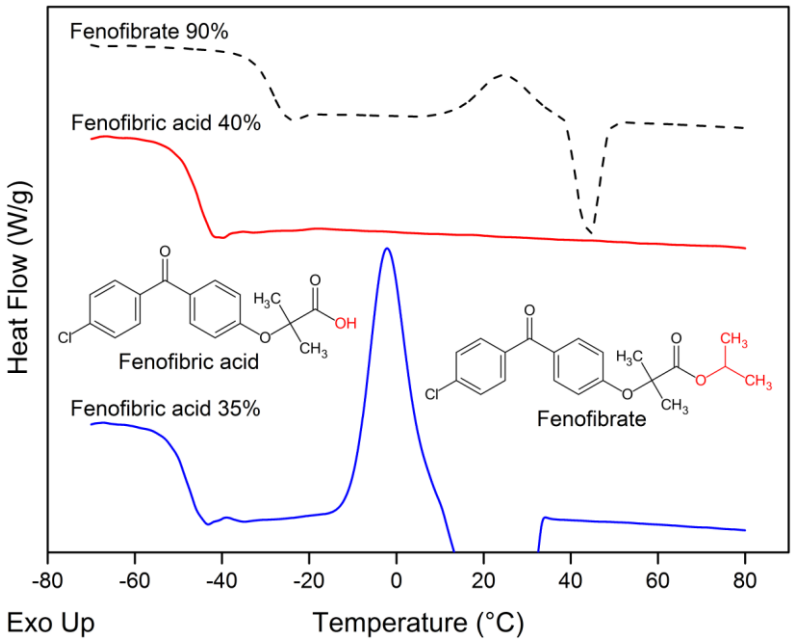

Figure 4. DSC thermograms with heat flow signal *vs*. temperature for dispersions of PEG and fenofibrate and its hydrolyzed derivative containing different loadings.

Figure 4 depicts another example of the influence of hydrogen bonding on the crystallization inhibition effect of API on PEG as studied by DSC. Fenofibrate contains only proton acceptor groups and the API is therefore impossible to interact with PEG via hydrogen bonding. Consequently, this compound lacks the inhibition effect on the PEG crystallization process as exhibited by the crystallization and melting peak of PEG in dispersions containing up to 90% of drug loading. In contrast, the hydrolyzed derivative of fenofibrate showed a totally different

behavior: fenofibric acid is a surprisingly strong crystallization inhibitor of PEG with the complete polymer amorphization observed at as low as 40% weight fraction. The hydrolysis process of fenofibrate to obtain fenofibric acid is supplied in **Supporting information**, section S3.

These examples clearly demonstrate that compounds that can form interactions with PEG are able to retain the amorphous nature of the polymer in their dispersions whereas non-interacting additives are unable to inhibit the crystallization of PEG. In order to verify the presence or absence of drug-carrier interactions in these systems, various spectroscopic techniques have been applied as outlined below.

FTIR Spectroscopic Investigation of PEG-IMC Interactions

IMC exists in various monotropic polymorphs, namely α, β, γ, δ, ε, ζ, η as well as an unnamed crystal form;[24-26] the γ form is the stable form. XRD data show that the raw material of IMC was the γ form and it was transformed into the α polymorph in solid dispersions with PEG (data not shown), thus α-IMC will be used as a reference to analyze FTIR spectra of its PEG-based solid dispersions.

Due to the fact that PEG and polymorphs of IMC exhibited very broad OH vibration bands between 3400 to 2500 cm^{-1} and this stretching region was superimposed on the CH bands (See **Supporting information**, Figure S2), it was troublesome to detect any changes in this region. Therefore, only the carbonyl stretching vibration region from 1800 to 1600 cm^{-1} was examined to identify any interactions between IMC and PEG.

It is known from single crystal structure data that γ-IMC forms cyclic dimers between carboxylic acid groups with one pair of molecules packed in an asymmetric unit,[27] so that the vibration at 1713 cm^{-1} must correspond to the asymmetric stretch of acid carbonyl of the dimer (Figure 5). The band at 1690 cm^{-1} is assigned as benzoyl carbonyl. α-IMC exists as chains of molecules interacting through the acid moiety with a set of three crystallographically

inequivalent molecules per unit cell in which two molecules form a hydrogen bonded carboxylic acid dimer, while the carboxylic acid of the third molecule is hydrogen bonded to one of the amide carbonyls of the dimer.[28] Both vibrations at 1680 and 1649 cm^{-1} are assigned to hydrogen bonded acid carbonyl of the dimer while non-hydrogen bonded acid carbonyl group at the end of molecular chains could account for the weak peak at 1734 cm^{-1}; the band at 1691 cm^{-1} corresponds to the benzoyl carbonyl stretching. Amorphous IMC consists mainly of cyclic dimers with a small fraction of molecules hydrogen bonded to form a chain,[29, 30] thus vibration bands of both asymmetric acid carbonyl of cyclic dimer at 1707 cm^{-1} and non-hydrogen bonded acid carbonyl stretch at 1735 cm^{-1} are detectable. Benzoyl carbonyl vibration shows a band at 1679 cm^{-1}.[29] PEG displays no peak in the carbonyl stretching region.

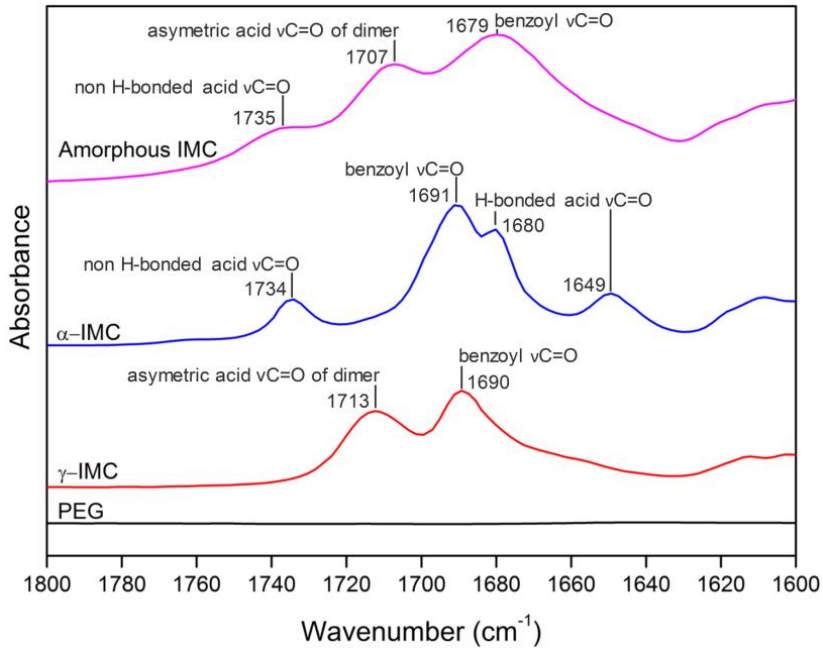

Figure 5. FTIR spectra of PEG, γ-IMC, α-IMC and amorphous IMC in the spectral region between 1800-1600 cm^{-1} at room temperature.

In the solid state, after almost 1 year of storage at room temperature, the formation of solid dispersions with PEG did not modify any peak position in the FTIR spectrum of α-IMC, indicating the absence of any specific interactions between the two components (Figure 6A). This is strongly consistent with the data reported in literature.[15-17] At 165°C which is above the

melting points of γ-IMC (161°C) and PEG (60°C), the dispersions exist in the liquid (molten) state and exhibit two remarkable changes in their FTIR spectra (Figure 6B).

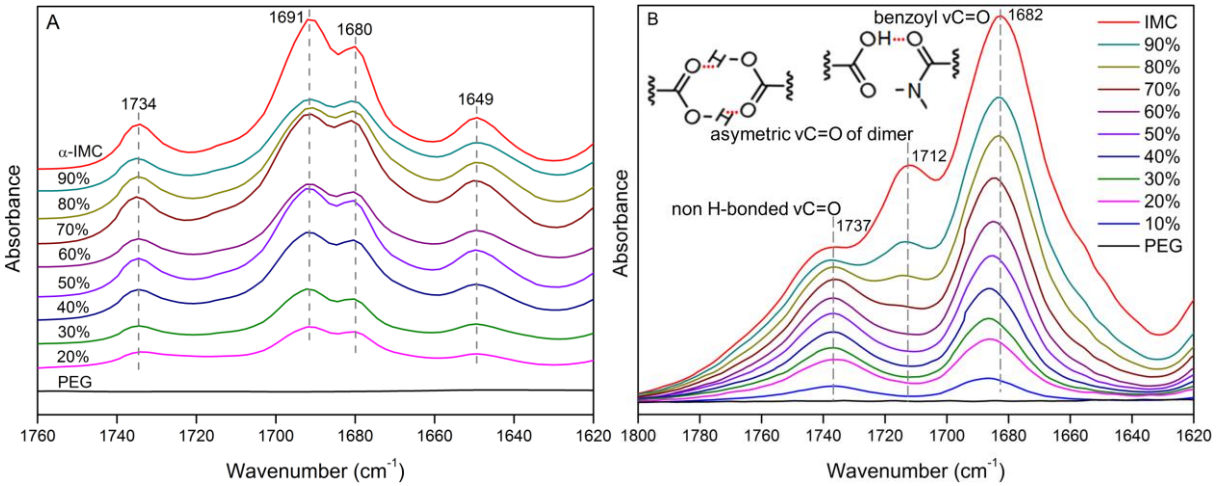

Figure 6. FTIR spectra of the carbonyl stretching region of PEG, IMC and their dispersions containing different drug loadings in (A) solid state at room temperature and (B) liquid state at 165°C.

Firstly, the asymmetric carbonyl stretching vibration of IMC cyclic dimer at 1712 cm^{-1} significantly decreased in intensity with the reduction of drug loading before this band completely disappeared in dispersions containing 50% IMC. The presence of polymer has displaced IMC self-interactions in the cyclic dimer by drug-polymer interactions and the disruption effect reached the highest level at the weight fraction of 50% PEG where the amount of polymer was sufficient to entirely disrupt IMC dimers. Secondly, the benzoyl carbonyl band of IMC at 1682 cm^{-1} remarkably shifted to higher wavenumber as the polymer content increased. Yuan et al.[30] recently demonstrated that 19% of amorphous IMC was hydrogen bonded through its carboxylic acid and benzoyl carbonyl groups. Therefore, the increase in wavenumber of the benzoyl carbonyl stretching vibration could be attributed to the conversion of this functional group from hydrogen bonded to non-hydrogen bonded in the presence of PEG.

Temperature-variable FTIR Spectroscopic Investigation of PEG-IMC Dispersions

It must be noted that at 165°C, vibrational bands of amorphous IMC in the carbonyl stretching region appear at higher wavenumbers compared to those at room temperature. The peak positions at room temperature of the benzoyl carbonyl at 1679 cm^{-1}, asymmetric carbonyl of the cyclic dimer at 1707 cm^{-1} and the non-hydrogen bonded carbonyl at 1735 cm^{-1} (Figure 5) shifted to 1682, 1712 and 1737 cm^{-1}, respectively when the temperature increased to 165°C (Figure 6B). To gain further insight into spectroscopic behavior of IMC, temperature-variable FTIR spectroscopy was utilized.

Figure 7 shows the temperature-dependent FTIR spectra of IMC and its 70% dispersions with PEG in the temperature range from 40 to 180°C. For pure amorphous IMC (Figure 7A), the stretching vibration bands of the benzoyl carbonyl at 1681 cm-1 and cyclic dimer carbonyl at 1707 cm-1 at 40°C shifted to higher wavenumber as temperature increased as a result of the disruption of hydrogen bonds whereas the position of the non-hydrogen bonded carbonyl stretching vibration remained more or less constant at 1734 cm^{-1}.

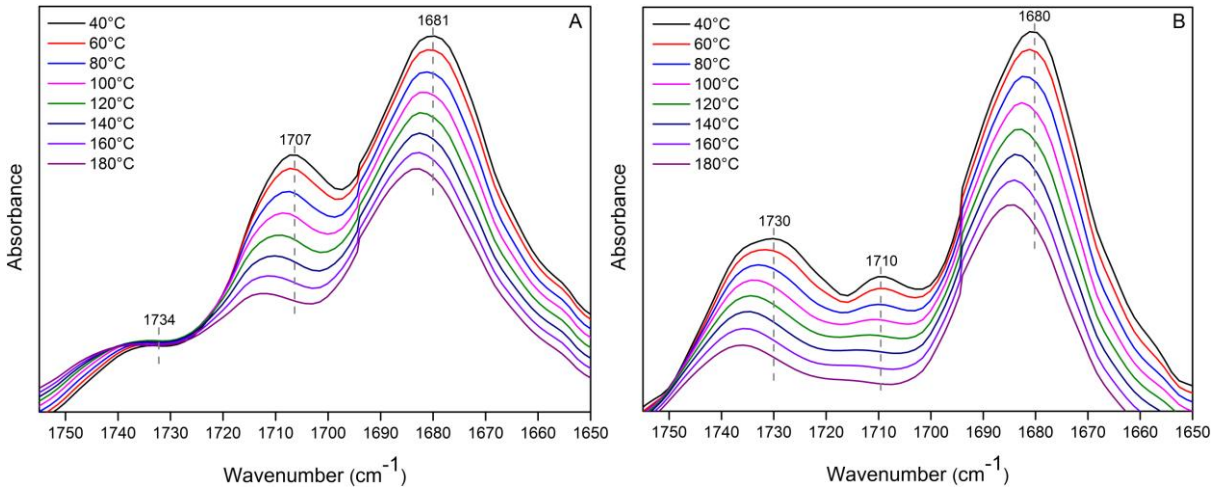

Figure 7. FTIR spectra as a function of temperature of the carbonyl stretching region of (A) IMC and (B) PEG/IMC dispersions containing 70% IMC.

In the presence of 30% weight fraction of PEG (Figure 7B), heating led to a shift of the benzoyl carbonyl and non-hydrogen bonded carbonyl bands to higher wavenumbers while the stretching

vibration of the carbonyl of the cyclic dimer at 1710 cm^{-1} diminished rapidly in intensity due to the disappearance of hydrogen bonds between drug molecules. The disruption of the cyclic dimer of IMC in dispersions with PEG was much faster than that in pure amorphous IMC upon increasing temperature, suggesting that the presence of PEG was an additive driving force to the heat to break up drug self-hydrogen bonding to form drug-carrier interactions.

At 165°C, the peak position of the non-hydrogen bonded carbonyl stretching vibration band of IMC did not seem to be affected, regardless of the amount of PEG in the dispersions (Figure 6B), indicating the absence of hydrogen bonding between the hydroxyl end group of the polymer with carbonyl groups of IMC. Consequently, the drug-carrier interactions must be between the hydroxyl moiety of IMC and the ether oxygen of PEG. This reasoning is compatible with the limited number of hydroxyl end groups of PEG in comparison with the abundance of ether oxygens.

Unfortunately, the stretching vibration region of the hydroxyl group of IMC is too broad (Figure S1) and hinders the identification of any changes in this region as a result of hydrogen bonding. Therefore, the more sensitive spectroscopic technique ^{13}C NMR[31-34] will be employed to further probe specific PEG-IMC interactions.

NMR Spectroscopic Investigation of PEG-IMC Interactions

Figure 8 shows ^{13}C CP/MAS NMR spectra of α-IMC, PEG and their solid dispersions containing 1:1 molar ratio of IMC to PEG monomer. As depicted by the figure, α-IMC exhibited signals being split into three peaks for most carbons, which could be explained by the presence of three types of conformationally different molecules packed in an asymmetric crystalline unit cell. The peaks of α-IMC have been previously assigned.[35, 36] Apparently, after approximately 1 year of storage at room temperature, there was no change in the signals of α-IMC in the solid dispersions compared to those of the pure drug, indicating the absence of any specific

interactions between IMC and PEG in the solid state, hence confirming FTIR results and previous studies.[15-17]

Pure PEG showed a broad peak at 71.5 ppm which is composed of a sharp resonance of highly mobile PEG in amorphous domains at 70 ppm, superimposed on a broad resonance corresponding to PEG in crystalline domains centered at 72 ppm.[37] The broadening of the resonance of crystalline PEG results from the interference of the decoupling field frequency and the frequency of rotational oscillation of PEG helices.[38] In solid dispersions with IMC, the PEG signal appears at 71.0 ppm and becomes much sharper, suggesting signifcantly decreased crystallinity of PEG in the presence of IMC.

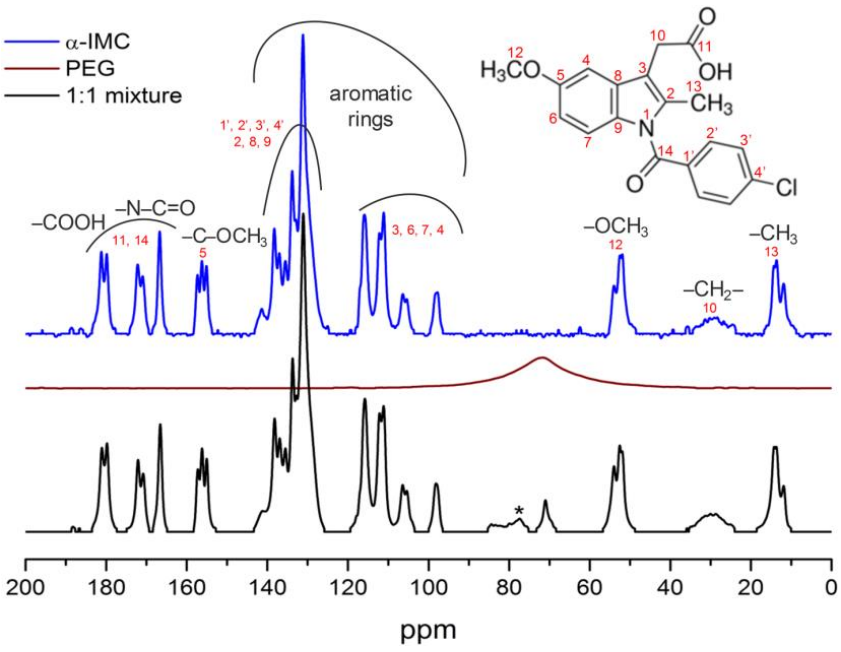

Figure 8. ^{13}C CP/MAS NMR spectra at room temperature of α-IMC, PEG and their solid dispersions containing 1:1 molar ratio of IMC to PEG monomer units after *ca.* 1 year of storage at room temperature. Asterisk denotes a spinning sideband.

While IMC and PEG showed no specific interactions in the solid state, IMC self-hydrogen bonding was being disrupted and displaced by drug-polymer interactions in the liquid state as previously described by the FTIR data. The evidence of interactions between IMC and PEG in their liquid mixtures can be found in ^{13}C NMR spectra as demonstrated in Figure 9.

In this set of experiments, solid dispersions of IMC and PEG were carefully packed in NMR rotors and heated at 165°C in an oven to obtain the molten mixtures before cooling to ambient temperature. The samples were then reheated during NMR measurements. Ideally, the measuring temperature should be maintained at 165°C to ensure no crystallization during the experiments, yet this temperature is much higher than the working limit of the equipment and extremely risky because spinning of the molten samples at high rate might push out the rotor cap. For those reasons, the temperature was kept at 75°, which is *ca*. 20°C and 30°C above the melting point of PEG and the glass transition temperature of IMC, respectively. At this temperature, the drug and polymer exist as a liquid mixture.

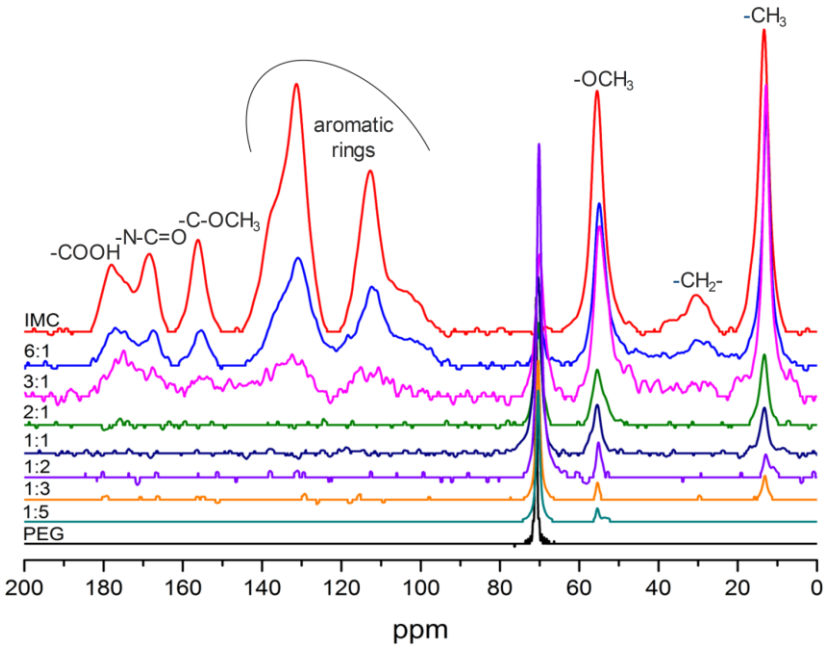

Figure 9. ^{13}C CP/MAS NMR spectra of amorphous IMC, PEG and their dispersions containing different molar ratios of IMC to PEG monomer units at 75°C.

IMC showed much broader peaks in these samples compared to those of the crystalline α-polymorph, indicating the amorphous nature of the drug (Figure 9). Only the methyl and methoxy signals were rather sharp due to fast rotation. In molten dispersions at 75°C containing a 1:1 ratio of IMC to PEG monomer units, all IMC ^{13}C NMR signals between 90-180 ppm

became undetectable. Only the sharp methyl and methoxy signals were still weakly observed. This can be explained by the loss of cross-polarization efficiency in the mobile IMC molecules upon attachment to polymer chains via hydrogen bonding. Only carbon resonances having a relatively high number of protons *i.e.* of the methoxy groups at 55.4 ppm and methyl groups at 13.3 ppm can be observed despite of the weak cross-polarization efficiency. The same phenomenon was already observed for 2:1 molar ratio dispersions, suggesting that each oxygen of a PEG unit can form hydrogen bonds with two IMC molecules.

In molten mixtures containing more IMC *e.g.* molar ratios of 3:1 and 6:1, the number of drug molecules was larger than the number of hydrogen bonding forming oxygen centers of the polymer and the excess of IMC was not involved in hydrogen bonding with PEG. These non-interacting drug molecules have lower rotational mobility and can be cross-polarized more efficiently than the interacting ones, explaining why the ^{13}C NMR signals of the resulting free IMC become much stronger and visible in the range from 90-180 ppm. In contrast, the signals of IMC in samples containing higher amounts of polymer *e.g.* 1:2, 1:3 and 1:5 were continuously decreasing in intensity before vanishing due to the dilution effect (Figure 9). For NMR measurements using direct polarization, the IMC signals in this kind of samples can always be easily detected (**Supporting information**, Figure S3), confirming the cross-polarization-driven changes in IMC signal intensity.

While the intensity of IMC signals was largely dependent on the ratio of IMC to PEG monomer, the resonance of PEG at 71.0 ppm shifted upfield with increasing drug concentration, indicating that the methylene groups of PEG which are in interaction with IMC appear in the shielding region of the hydrogen bond donating carboxylic groups of IMC. Additionally, the PEG signals also became broader, owing to the lower mobility of the polymer in more viscous and highly drug-concentrated mixtures (Figure 10).

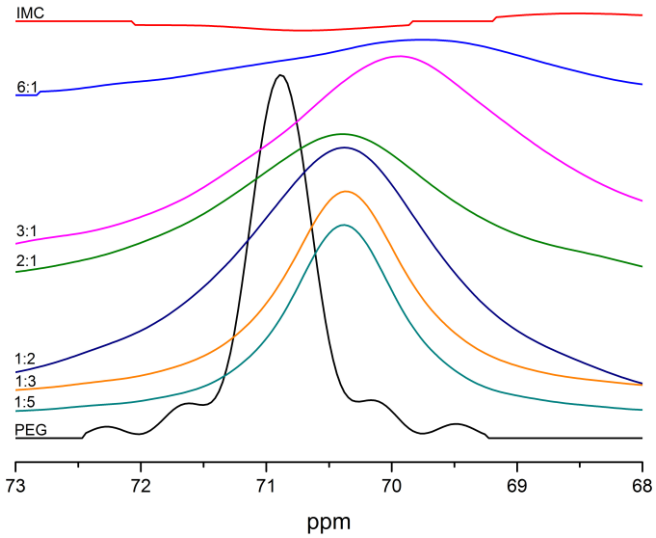

Figure 10. ^{13}C CP/MAS NMR spectra of PEG in dispersions containing different ratios of IMC to PEG monomer units at 75°C.

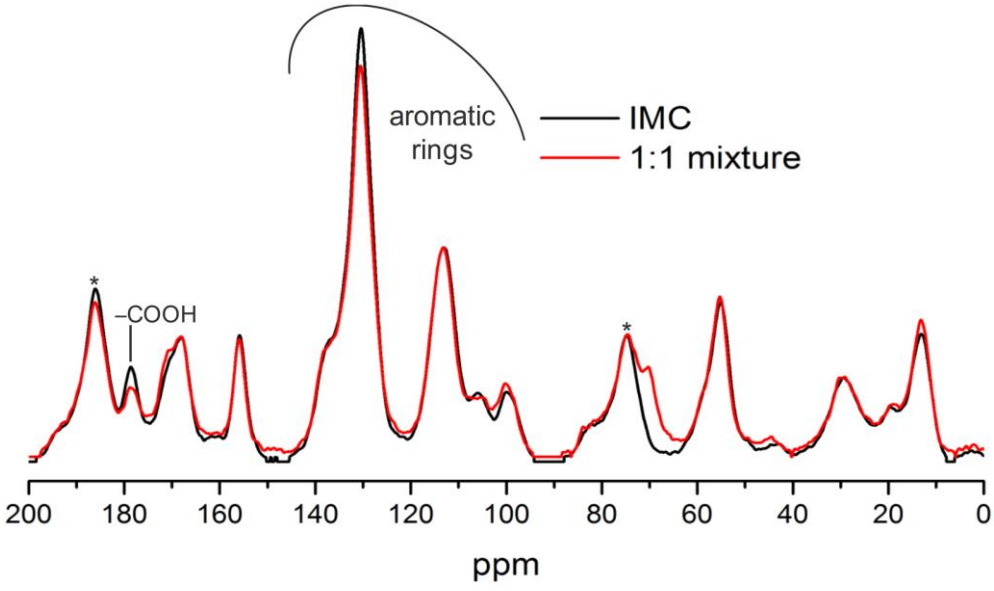

Figure 11. ^{13}C CP/MAS NMR spectra at room temperature of IMC and its dispersion with PEG in a 1:1 molar ratio of IMC to PEG monomer units within 1 hour of solidification from the melt. Asterisks denote spinning sidebands. The spinning rate was increased to 5600 Hz to avoid overlap between the spinning sidebands and the carboxylic acid resonance of IMC.

Immediately after solidification from the melt, the 1:1 dispersions still remained in the amorphous state and the IMC signals became much more intense than at 75°C owing to the improved cross-polarization efficiency due to the lower drug molecular mobility (Figure 11). As compared to solidified IMC, only small changes were observed for the peaks corresponding to the carboxylic group at 178.8 ppm and the aromatic ring at 130.6 ppm, most likely due to the hydrogen bonding with the polymer.

The Disruption of PEG-IMC Interactions upon Storage

The interactions between IMC and PEG were further monitored upon solidification. During storage, due to the crystallization of PEG, the drug-polymer interactions will be disrupted and displaced by self-interactions of IMC molecules that form cyclic dimers and molecular chains via hydrogen bonding before amorphous IMC crystallizes to the α-form. Figure 12 displays time-resolved FTIR spectra of 60 weight% IMC dispersions with PEG upon storage at room temperature.

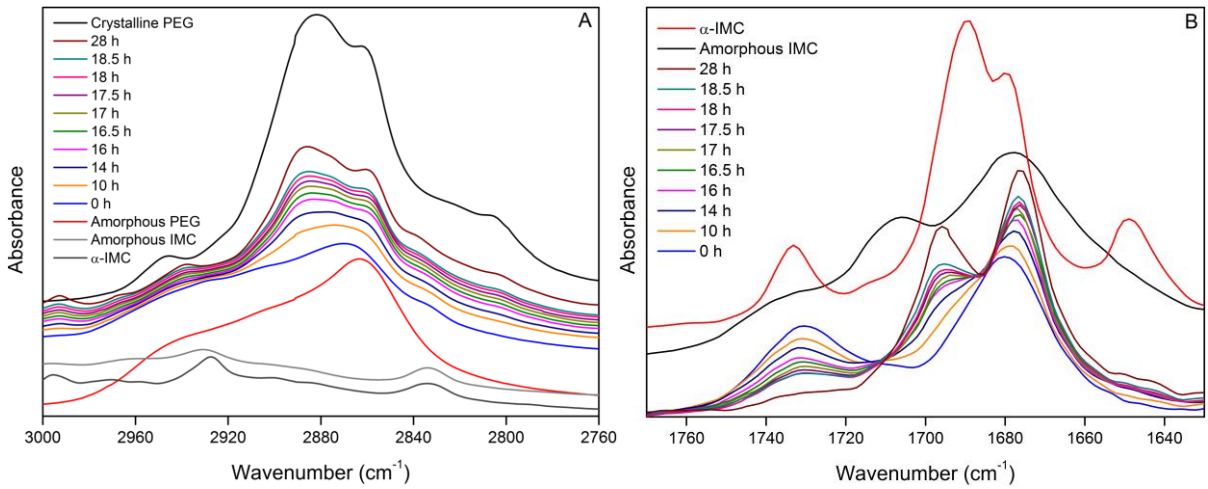

Figure 12. FTIR spectra of (A) CH and (B) carbonyl stretching region of PEG/IMC dispersions containing 60 weight% IMC as function of storage time at room temperature.

Initially, IMC showed a negligible stretching vibration band of cyclic dimer carbonyl (Figure 12B). This vibration evolved rapidly and then became significantly evident at *ca*. 1693 cm^{-1}

after 14 hours when amorphous PEG in the dispersions began to transform into the crystalline state as can be seen in Figure 12A. The band continued to develop upon storage. Meanwhile, the stretching vibration of the benzoyl carbonyl at *ca*. 1678 cm^{-1} was increasing in intensity and shifting to lower wavenumber whereas the vibration corresponding to the non-hydrogen bonded carbonyl at 1731 cm^{-1} stayed at the same position but was significantly decreased in intensity, both due to the formation of hydrogen bonds between free drug molecules. The data demonstrate that the hydrogen bond formation and disruption in the dispersions of IMC and PEG are reversible.

Spectroscopic Investigation of Interactions between PEG and IMC Derivatives

As previously illustrated in Figure 3, the methoxy ester derivative of IMC was unable to inhibit the crystallization of PEG at any drug loading. One might reason that the absence of the crystallization inhibition effect is due to the absence of hydrogen bonding with the polymer because the methoxy ester of IMC does not contain proton donating groups to interact with the ether oxygen of PEG.

This idea was confirmed by FTIR data (Figure 13). Evidently, the formation of both solid and liquid dispersions with PEG did not lead to any changes in the carbonyl vibration region of the IMC methoxy ester, indicating the absence of any specific drug-polymer interactions. This was further verified by ^{13}C NMR. Figure 14 shows the ^{13}C CP/MAS NMR spectra of molten dispersions of IMC methoxy ester in PEG. No modifications in terms of both chemical shift and intensity could be detected, demonstrating a non-interacting mixture. This also rejects the interaction between the hydroxyl end groups of PEG with the carbonyl moiety of IMC.

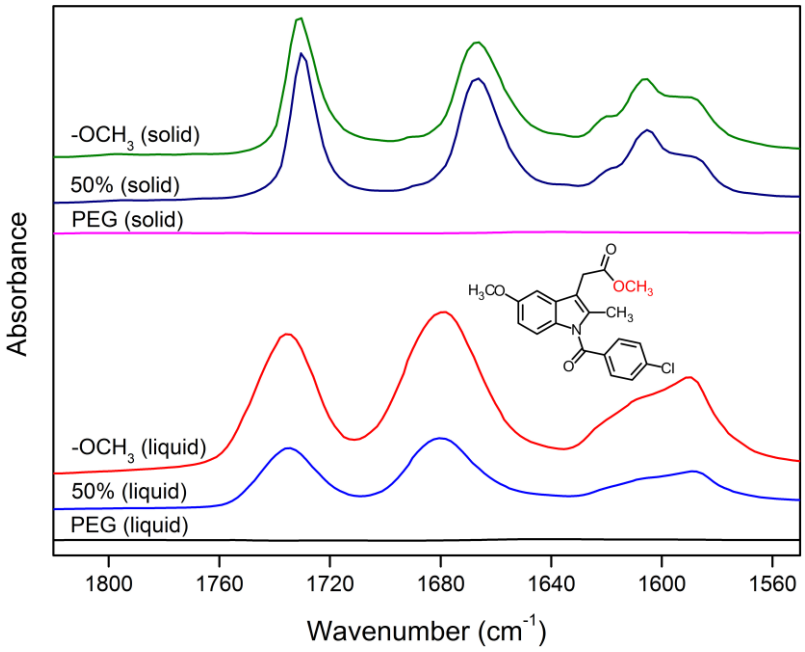

Figure 13. FTIR spectra of the carbonyl stretching region of the dispersion of PEG and IMC methoxy ester in the solid state at room temperature (top) and in the liquid state at 100°C (bottom). The melting point of IMC methoxy ester is *ca*. 91°C.

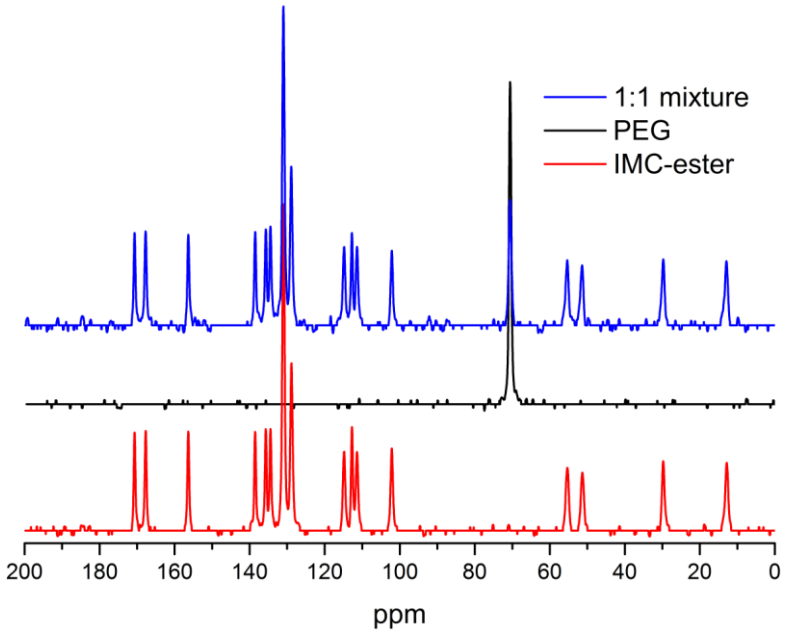

Figure 14. ^{13}C CP/MAS NMR spectra of dispersions of PEG and IMC methoxy ester containing a 1:1 molar ratio of IMC derivative to the PEG monomer units in the liquid state at 100°C. The contact time for cross-polarization was set at 6 ms to acquire stronger signals.

For another derivative of IMC, the DSC data showed that when the carboxylic hydroxyl moiety of IMC was substituted by an amide group, the new compound could still effectively inhibit PEG crystallization as shown in Figure 3. The preservation of the polymer crystallization inhibition effect of the amide derivative could be attributed to the interactions between the two components via the donation of a hydrogen bond from the amide moiety of the derivative to the PEG ether acceptor group.

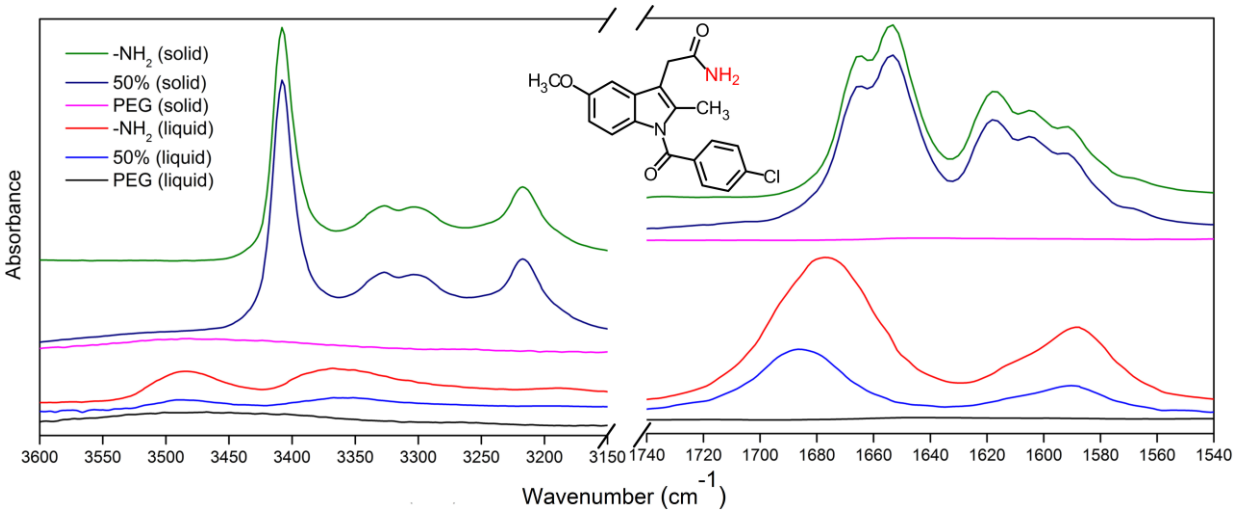

Figure 15. FTIR spectra of the carbonyl and amide N-H stretching region of dispersions of PEG and the amide derivative of IMC in solid state at room temperature and in liquid state at 230°C. The melting point of the amide derivative of IMC is *ca.* 220°C.

Figure 15 shows the FTIR carbonyl and amide stretching regions of dispersions of PEG and the amide derivative of IMC in the molten and solid state. Primary amides have been reported to form preferred hydrogen-bond motifs involving cyclic dimers and chains[39, 40] which are partially breaking up on melting producing weakly linked molecules.[41] Accordingly, in the liquid state, the vibration of the liquid IMC derivative at 1589 cm^{-1} (red curve) is assigned as dimer carbonyl while the band at higher wavenumber of 1677 cm^{-1} must correspond to the stretching vibration of the hydrogen bonded benzoyl carbonyl.

Following the formation of molten dispersions with PEG (blue curve), both carbonyl bands shifted to higher wavenumbers, indicating the disruption of the IMC derivative intermolecular

interactions to form hydrogen bonding between the amide moiety of the derivative and the ether oxygen of PEG. The positions of infrared peaks in the amide stretching region are more or less unchanged. Upon solidification, the FITR patterns of the amide derivative of IMC in the dispersions with PEG and those of the pure derivative are exactly the same, demonstrating the disappearance of heteromolecular interactions in the solid state.

FTIR Spectroscopic Investigation of PEG-APIs Interactions

FTIR spectroscopy was applied with a view to verify if interactions pattern in dispersions of PEG with IMC and its derivatives can be found in other PEG-APIs dispersions. Fenofibrate showed no crystallization inhibition effect on PEG as described earlier in Figure 4. This discrepancy was evidently associated with the absence of any drug-polymer specific interactions between fenofibrate and PEG in their dispersions in not only solid but also liquid state (Figure 16). It is obvious that the stretching vibration bands of fenofibrate including ester carbonyl on the left and ketone carbonyl in the middle[42] were all unaltered in the presence of PEG. The signals on the right are assigned to in-plane benzene ring stretching vibrations.

Interestingly, the hydrolyzed product of fenofibrate which is fenofibric acid acted as a powerful crystallization inhibitor for PEG (Figure 4). Based on the data obtained for other APIs, one might rationally attribute this to its interactions with PEG. Figure 17 shows the partial FTIR spectra of dispersions of PEG and fenofibric acid in liquid and solid state. Being a monocarboxylic acid, fenofibric acid molecules may link to each other by hydrogen bonds into cyclic dimers, catamers (linear chains) or heterogenic associations involving the hydroxyl moiety and ketone carbonyl.[40, 43, 44] The formation of dispersions with PEG in liquid state results in the displacement of drug-drug interactions by drug-polymer interactions that in turn leads to the shift of carbonyl stretching vibrations. Similar to the aforementioned PEG-APIs mixtures, the specific interactions between fenofibric acid and PEG vanished upon solidification of the dispersions.

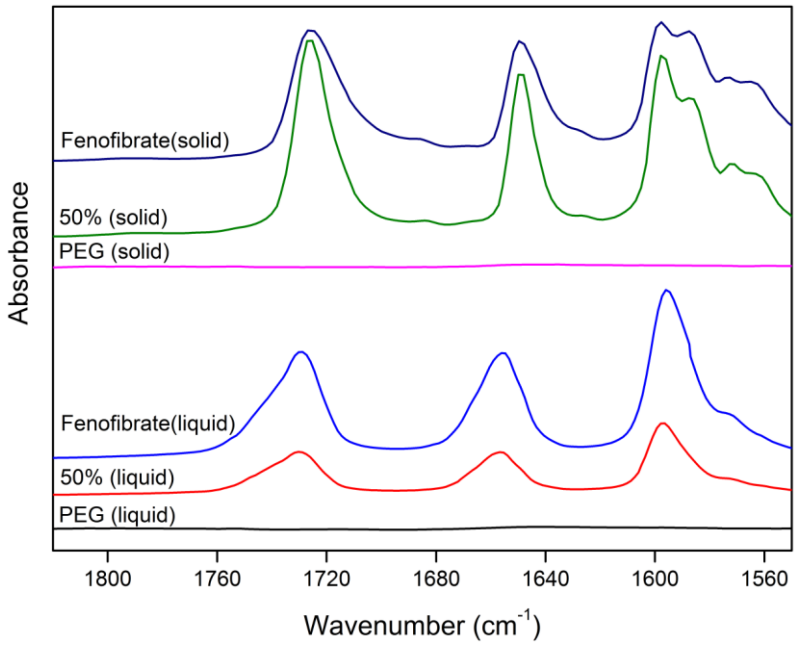

Figure 16. FTIR spectra of the carbonyl stretching vibration region of dispersions of PEG and fenofibrate in solid state at room temperature and in liquid state at 90°C. The melting point of fenofibrate is *ca*. 81°C.

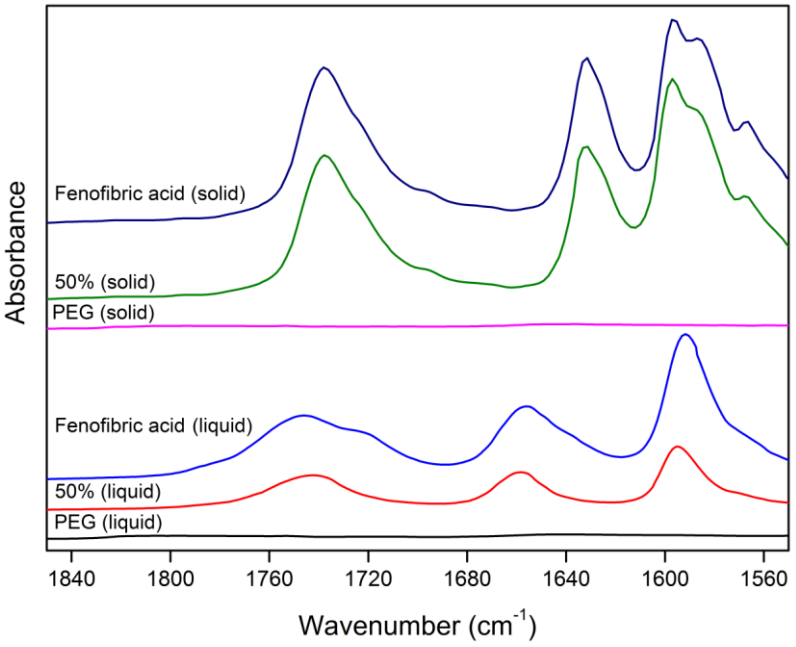

Figure 17. FTIR spectra of the carbonyl stretching vibration region of dispersions of PEG and fenofibric acid in solid state at room temperature and in liquid state at 190°C. The melting point of fenofibric acid is *ca*. 180°C.

The spectroscopic investigations yielded a universal and consistent result that all PEG crystallization inhibitors can interact with PEG in their liquid dispersions whereas compounds which do not form interactions with the polymer are unable to maintain the amorphous nature of PEG. Furthermore, the drug-carrier interactions disappeared upon solidification, regardless of the interaction pattern in the molten mixture.

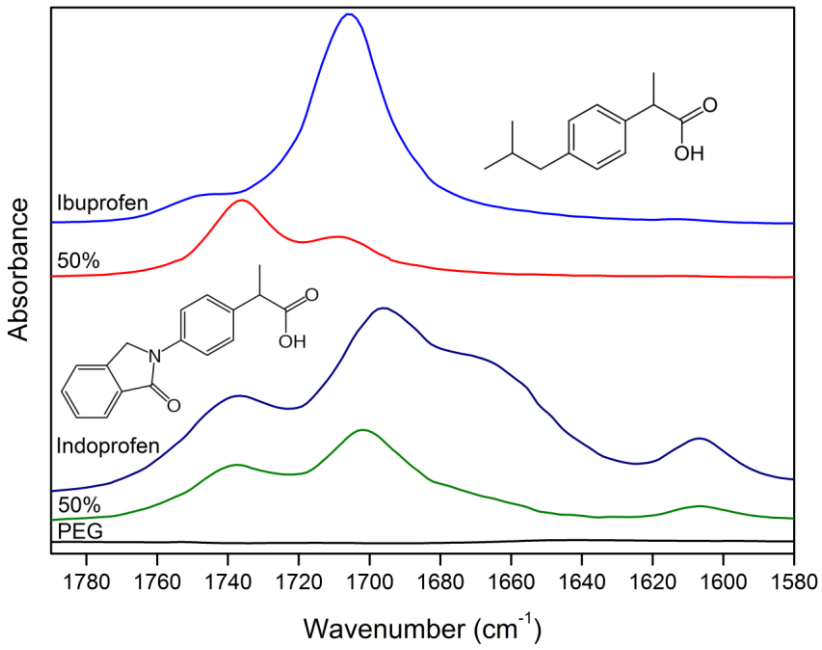

Figure 18. FTIR spectra of the carbonyl stretching region of dispersions of PEG with ibuprofen and indoprofen at *ca*. 10°C above the melting point of the drugs, which are 85°C and 220°C, respectively.

However, many APIs contain carboxylic acid groups that can interact with PEG like IMC, yet their inhibition effect on PEG crystallization is absent. As illustrated in Figure 18, stretching vibrations of ibuprofen and indoprofen in the carbonyl stretching region significantly shifted to higher wavenumbers in dispersions with PEG due to the disruption of drug-drug interactions to form drug-polymer hydrogen bonding. However, PEG still crystallizes extremely rapidly in dispersions with both compounds, demonstrating the inability of these drugs to inhibit the crystallization of the polymer despite of substantial drug-polymer hydrogen bonding.

Accordingly, the interactions between APIs and PEG is a necessary but not sufficient condition for the polymer crystallization inhibition effect.

The Influence of Polymer Molecular Weight on the Crystallization Inhibition Effect of IMC

Due to the fact that molecular weight of PEG may govern various properties of the polymer including crystallinity,[45] crystallization rate,[14, 46, 47] drug-polymer miscibility[48] and microstructure,[45] it is worthwhile elucidating whether the crystallization inhibition effect of APIs depends on polymer molecular weight. The DSC data demonstrated that there was almost no difference in the crystallization inhibition behavior of IMC on PEG when the polymer molecular weight varied from 4000 to 6000, 20,000, 100,000 or even 8,000,000 Dalton. In this wide range of molecular weight, the same drug loading of 50 – 55% IMC was required to maintain the polymer in the amorphous state during DSC measurements (data not shown).

The Crystallization Inhibition Effect of IMC on Other Semi-crystalline Polymers

The effect of IMC and other PEG crystallization inhibitors on the crystallization process of other semi-crystalline polymers like different types of poloxamer and Gelucire 44/14® has been also probed by DSC. The crystallization inhibition effect of APIs still exhibited in dispersions with the two polymers. For poloxamer, this effect was independent on the ratio of ethylene oxide and propylene oxide portion in the triblock copolymer as the crystallization of poloxamer 188, 338, 407 was completely impeded in samples containing the same amount of IMC of at least *ca*. 50% (data not shown).

DISCUSSION

Required Conditions for Polymer Crystallization Inhibition

The screening for PEG crystallization inhibitors discovered several candidates including ketoprofen, suprofen, tiaprofenic acid, flurbiprofen, fenoprofen, not to mention their amide

derivatives and fenofibric acid, suggesting that the PEG crystallization inhibition effect is a general characteristic of numerous APIs and not limited to IMC. These PEG crystallization inhibitors share a common structure which is a proton donating functional group like carboxylic or amide that can form hydrogen bonds with the ether oxygen of PEG. However, as discussed for ibuprofen and indoprofen, these two drugs also contain carboxylic groups and are able to interact with PEG as shown in FTIR spectra (Figure 18) but cannot maintain the amorphous nature of PEG. This indicates that hydrogen bonding is a necessary but not sufficient condition for the polymer crystallization inhibition.

The other condition might be the strength of PEG-API hydrogen bonds. When the carboxylic moiety of IMC was substituted by an amide group, the difference in the molecular weight between the two compounds (1 Dalton) is negligible. Nevertheless, 60% weight fraction of the amide derivative is needed to completely inhibit PEG crystallization whereas it is only 52% for IMC. Likewise, to prevent PEG from crystallization, the weight fraction required for ketoprofen and its amide derivative are 55% and 65%, respectively. This discrepancy can be attributable to the stronger hydrogen bonding capacity of the carboxylic group as compared to the amide group, which is in turn originating from higher electronegativity of the oxygen atom (3.5) than that of the nitrogen atom (3.0). The hydrogen bonding strength might also explain the absence of the PEG crystallization inhibition effect of ibuprofen: it is likely that the α-methyl group causes steric hindrance and by this obstructs optimal hydrogen bonding between ibuprofen and PEG.

Another factor that might contribute to the PEG crystallization inhibition by APIs is the crystallization tendency of the amorphous drugs. All crystallization inhibitors reported in this work belong to Class III, only flurbiprofen is found in Class II in the classification scheme of crystallization tendency of organic molecules proposed by Baird et al.,[49] meaning that these APIs have high glass forming ability. This is logical because if APIs are not able to maintain

their glassy state in dispersions with PEG but undergo fast crystallization, they cannot hydrogen bond with the polymer anymore and hence are impossible to inhibit polymer crystallization. This explains why indoprofen can form hydrogen bonding with PEG but does not act as a polymer crystallization inhibitor: it belongs to Class I in the crystallization tendency scheme that has low glass forming ability and the drug crystallizes extremely rapidly in dispersions with PEG upon solidification.

"Lock and Key" Model of Drug Molecules

We showed in Figure 9 that for the sample composed of a 2:1 molar ratio of IMC to PEG monomer units, no IMC ^{13}C NMR signal was detected anymore between 90-180 ppm due to the loss of efficient cross-polarization as a consequence of a too high mobility of IMC molecules upon adherence to PEG chains, suggesting that each PEG monomer unit could hydrogen bond to two IMC molecules. This is a striking observation because the 2:1 ratio of IMC to PEG monomer units corresponds to the 94:6 weight ratio, suggesting that only 6 weight% of PEG in the dispersions with IMC is already sufficient to eliminate the cross-polarization efficiency of IMC.

Due to the fact that the size of an IMC molecule is much larger than that of the PEG monomer, the attachment of two drug molecules to each ether oxygen may seem unlikely at first sight because of steric hindrance. Nevertheless, the perfect arrangement of IMC molecules along the polymer chains could be possible as a result of π-π stacking between aromatic rings of neighbouring IMC molecules as illustrated in Figure 19. Each IMC molecule can be considered as a combination of "lock and key" in which the aromatic ring is the "lock" that promotes π-π stacking to align the drug molecules parallel to each other and perpendicular to the polymer chains in order to minimize steric hindrance of the bulky moieties while the carboxylic acid group is the "key" that fastens the "locking" to the polymer chains via hydrogen bonding.

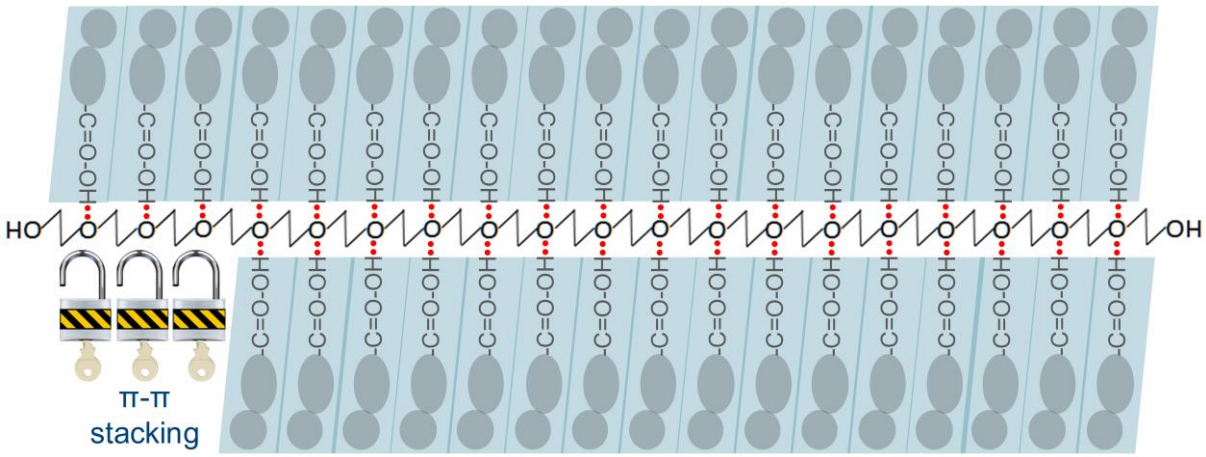

Figure 19. "Lock and key" model of drug molecules supports the formation of hydrogen bonds between IMC and PEG in dispersions containing a 2:1 molar ratio of IMC to PEG monomer units.

The Independence of Crystallization Inhibition Effect of Drug on Polymer Molecular Weight

Because hydrogen bonding plays a critical role in PEG crystallization inhibition, it is now unambiguous why the inhibition effect of APIs on PEG crystallization is independent on polymer molecular weight. Accordingly, it only depends on the molar ratio of API:PEG monomer or the number of hydrogen bond forming centers. IMC, for example, has a minimum inhibition concentration of *ca*. 50% regardless of polymer molecular weight, which is corresponding to a molar ratio of IMC to PEG monomer of approximately 1:8. Assuming that each IMC molecule forms a single hydrogen bond to one PEG oxygen in a 50 weight% IMC sample, the ratio 1:8 implies that in order to prevent PEG from crystallization, at least 1/8 of the monomer units of PEG must be involved in hydrogen bonding with IMC.

It has been found that crystalline PEG has a helical structure containing seven monomers with two turns per repeat unit in the fiber period of 19.3 Å[50] while in the molten state, the helical structure disintegrates to a completely disordered structure of random coils.[51] The crystallization of PEG from the melt therefore requires the folding of random coils into small

clusters before these clusters gather and coalesce into lamellae.[52-54] When 1/8 of the monomer units of PEG is locked in hydrogen bonding with IMC, no more than one repeat unit of helical structure can be folded, hence the polymer crystallization is completely inhibited.

Yang et al. explained this phenomena by the stiffness that prevents polymer chains from folding.[55] An apparent consequence of the role of hydrogen bonding in PEG crystallization inhibition by APIs is that increasing the drug loading will result in more PEG monomer units being blocked or in other words, the polymer chains become much stiffer. In addition, higher drug content leads to increased viscosity that restricts diffusional movements required for nucleation and crystal growth. For poloxamer, changing the ratio of ethylene oxide and propylene oxide co-monomer in this triblock copolymer does not result in a difference in the total number of hydrogen bond forming oxygen atoms, explaining that the crystallization inhibition effect of APIs on poloxamer is independent on the grade of this semi-crystalline carrier.

Reversible Formation and Disruption of Hydrogen Bonds

From the APIs viewpoint, it was found that *ca*. 50% IMC is needed to inhibit PEG crystallization. This value is well correlated with the drug loading for which the asymmetric carbonyl stretching vibration of the IMC cyclic dimer completely disappeared (Figure 6B). The presence of 50 weight% of the polymer is sufficient to fully displace IMC self-interactions by drug-carrier interactions, leading to the disappearance of the IMC cyclic dimer infrared band concurrently with the complete inhibition of polymer crystallization. Similarly, in solid dispersions with amorphous carriers such as poly(vinylpyrrolidone) and poly(vinylpyrrolidone-co-vinyl acetate), the fraction of IMC cyclic dimer always decreases as the polymer content increases before disappearing at a certain polymer weight fraction.[29, 30, 56]

The hydrogen bond formation and disruption in PEG-based solid dispersions is a reversible process. In the molten mixture, API self-interactions are displaced by drug-polymer interactions

while during solidification of the system, the pattern is opposite: the hydrogen bonds between API and PEG are displaced by drug self-interactions upon crystallization of PEG. During storage, when PEG starts to crystallize, the driving force for polymer chain folding has to be found in the disruption of hydrogen bonding between the API and PEG. Consequently, the API will be excluded from PEG crystals as a result of thermodynamic driving forces.

In addition to the fact that the entrapment of API in crystalline PEG is entropically unfavorable, the API itself also has a strong enthalpic driven tendency to crystallize, resulting in the rejection of the API from the PEG crystals.[57] The exclusion of amorphous API out of PEG crystals generates drug-rich domains, explaining the second T_g as illustrated in Figure 2. The high concentration of API in these domains in combination with its reduced T_g due to the presence of amorphous PEG with extremely low Tg will induce self-interactions between drug molecules and hence the nucleation and crystal growth of API crystals. The segregation of API from PEG crystals can be observed with polarized light microscopy (Figure 20). An overview of the formation and disruption of hydrogen bonds in PEG/API dispersions is illustrated in Figure 21. A similar process of reversible formation and disruption of interactions could also hold for amorphous dispersions.

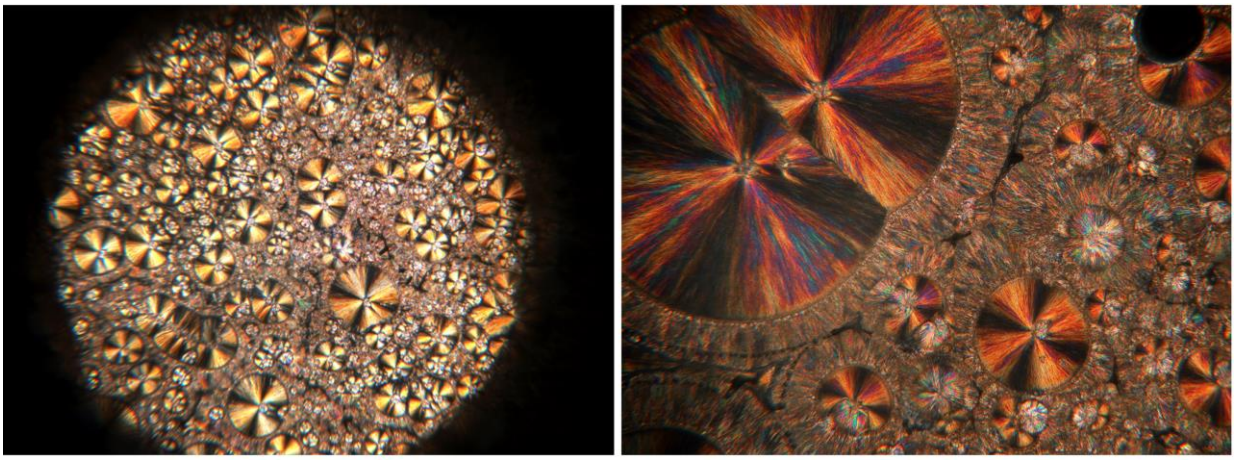

Figure 20. Polarized light microscopic illustration of the segregation of IMC from PEG crystals in solid dispersions containing 70% drug loading upon solidification.

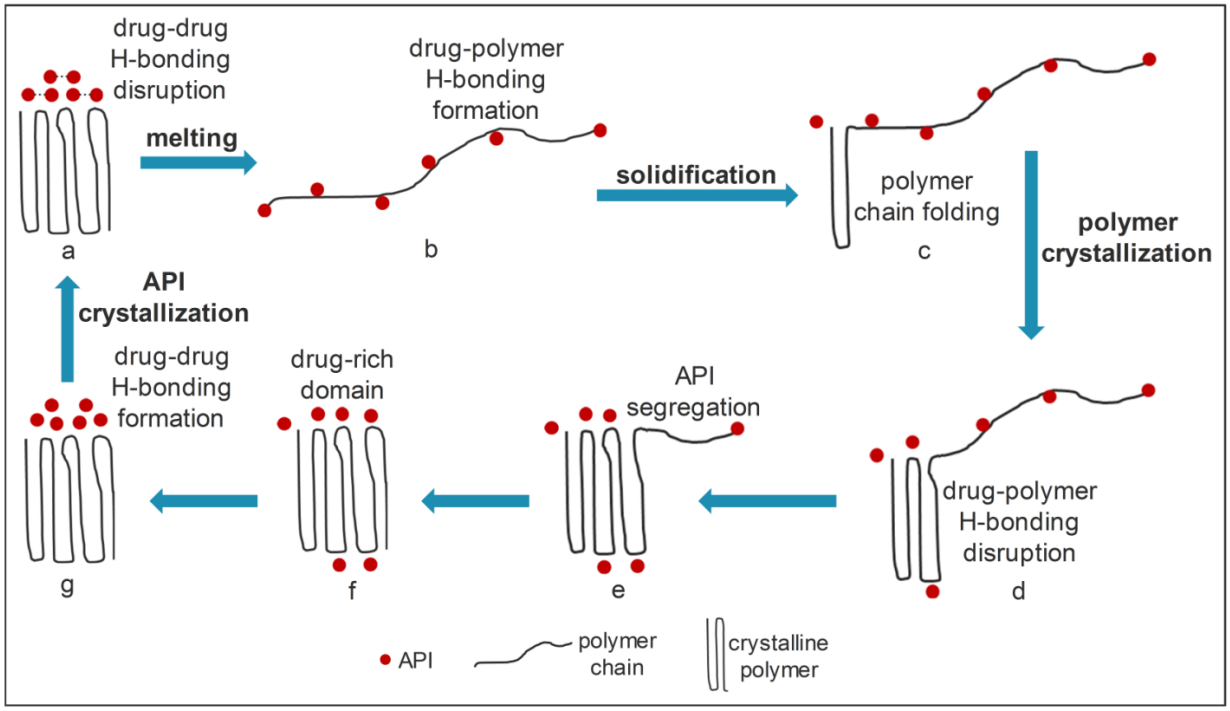

Figure 21. Overview of the formation and disruption of hydrogen bonds in PEG/API dispersions. (a) Crystalline PEG with folded chains and crystalline API with drug-drug hydrogen bonding. (b) In the molten mixture, PEG exists as completely disordered random coils. API self-interactions are disrupted and replaced by drug-polymer interactions. (c) Upon solidification, random coils of PEG fold into small clusters before these clusters coalesce into lamellae, resulting in polymer crystallization. (d) Polymer chain folding disrupts drug-polymer interactions. (e) Due to the disruption of hydrogen bonding between the drug and the polymer, the API is excluded from PEG crystals. (f) The segregation of amorphous API from PEG crystals generates drug-rich domains. (g) The formation of drug-drug self-interactions in drug-rich domains leads to the API crystallization.

Implications of Interactions on Physicochemical Properties of Dispersions

As discussed above, the drug-carrier interactions gradually become disrupted during storage, the rate and extent of which depend on the strength of the hydrogen bonding between API and PEG, on the interplay between drug-carrier and drug-drug interactions as well as on the

crystallization tendency of the carrier itself. The latter is dependent on polymer molecular weight, storage temperature, humidity, mechanical stress and other factors. As a consequence, the physicochemical properties and behavior of identical dispersions of PEG and API can be significantly different depending on how and how long they are stored, how much drug-carrier interactions are disrupted as well as on the degree of crystallinity of PEG and API in the samples. This might result and explain the discrepancy and irreproducibility in pharmaceutical performance of PEG-based solid dispersions both *in vitro* and *in vivo*. For example, Dubois and Ford reported the poor reproducibility of release rates from solid dispersions of PEG 6000 containing glutethimide[58] and phenylbutazone[15]. This research group also found that the dissolution from aged capsules containing temazepam and PEG 6000 prepared by liquid filling was erratic with high standard deviations.[59]

Furthermore, PEG-APIs specific interactions play a significant role in the formation and composition of an eutectic system. The interactions also dictate the effect of PEG molecular weight on the dissolution behavior of the incorporated drugs: APIs which exhibit specific interactions with the polymer have higher eutectic composition with and faster dissolution for lower molecular weight carrier while the molecular weight of PEG has no influence on the eutectic composition and dissolution profiles for compounds which do not interact with the polymer.[60] Considering the importance of drug-carrier interactions on the properties and performance of solid dispersions, the conclusion about the absence or presence of interactions between drugs and carriers must be made based on spectroscopic investigations of the systems not only in the solid state but also in the liquid or molten state.

It is interesting to note that IMC can inhibit the crystallization of PEG and reduce the crystallinity of the polymer not only immediately after preparation of the dispersions when drug-polymer interactions are detectable but also in the solid state after a long storage time during which the interactions were completely vanished. In a previous paper, we anticipated

that PEG exhibited biphasic crystallization behavior in dispersions with IMC with an initial fast phase within weeks and a second slow phase within months or years until its crystallinity reaches the value of the raw material of *ca*. 86%.[13] However, ^{13}C NMR data demonstrated that even after almost 1 year of storage, when no drug-carrier interactions can be detected, the crystallinity of PEG in dispersions with IMC is still much lower than that of the raw material.

Due to the fact that long PEG chains are not perfectly ordered, the resulting structure upon crystallization still contains fractions of amorphous material surrounding crystalline segments, making PEG a semi-crystalline carrier. The molecularly dispersed drugs reside predominantly in the amorphous PEG domains rather than in the crystalline moiety.[20, 61, 62] The presence of a fraction of IMC in the interphase will inhibit the crystallization of the polymer even without any interactions. In other words, these IMC molecules hinder the ordering of the polymer chains and induce defects in the PEG crystalline network, preventing it from growing. In the absence of IMC, molten PEG solidifies rapidly and its crystallinity increases to the extent of the raw material within weeks. Studying the microstructure of PEG-IMC solid dispersions *e.g.* by small angle X-ray scattering might provide insights into this phenomenon.

CONCLUSIONS

In this study, the formation and disruption of interactions in PEG-based dispersions have been well-characterized by spectroscopic methods. FTIR and NMR spectroscopy revealed strong PEG-IMC interactions in their liquid dispersions. Hydrogen bonding between the two components plays a critical role in the crystallization inhibition effect of IMC on PEG. IMC is also able to inhibit the crystallization of other semi-crystalline polymers such as poloxamer and Gelucire®. The screening of crystallization inhibitors for semi-crystalline polymers resulted in numerous candidates that exhibit the same behavior as IMC, demonstrating a general pattern of polymer crystallization inhibition. However, hydrogen bonding is a necessary but apparently

not a sufficient condition for the polymer crystallization inhibition: APIs should also have high glass forming ability to interact with the carrier and the drug-carrier interactions must be strong enough to hinder the polymer from crystallization. The PEG crystallization inhibition by drugs is independent on polymer molecular weight; it only depends on the amount of hydrogen bond formation *i.e.* the molar ratio of drug to PEG monomer units. In the molten mixture, each PEG monomer unit could form hydrogen bonds with two IMC molecules, possibly due to the perfect arrangement of drug molecules along the carrier chains that in turn is originating from π-π stacking between the aromatic rings of neighbouring IMC molecules. The interactions between API and PEG become weaker and disrupted upon solidification that results in the exclusion of the API from PEG crystals, indicating the reversibility of formation and disruption of hydrogen bonds in solid dispersions. The physicochemical properties and pharmaceutical performance of PEG-based solid dispersions depend on how and how long the samples are stored, how much drug-carrier interactions are disrupted as well as on the crystallinity of both drugs and the carrier. These mechanistic findings elucidate the discrepancy in physicochemical properties of PEG-based solid dispersions reported in the literature and are of great importance for preparation of solid dispersions with consistent and reproducible performance.

ASSOCIATED CONTENT

Supporting Information

The Supporting Information is available free of charge on the ACS Publications website at: http://pubs.acs.org.

AUTHOR INFORMATION

Corresponding Author

*E-mail: Guy.VandenMooter@pharm.kuleuven.be. Tel.: +32 16 330 304. Fax: +32 16 330 305.

Author Contributions

The manuscript was written through contributions of all authors. All authors have given approval to the final version of the manuscript.

Notes

The authors declare no competing financial interest.

ACKNOWLEDGEMENTS

The authors would like to acknowledge the financial support from Research Foundation Flanders (FWO-Vlaanderen). Tu Van Duong gratefully acknowledges the scholarship (G.0764.13) and travel grant (K1H0416N) awarded by FWO-Vlaanderen. Peter Adriaensens wants to thank the FWO-Vlaanderen for supporting the scientific research community project MULTIMAR (Multidisciplinary Magnetic Resonance). We thank Dr. Pieterjan Kayaert, Amatsigroup and Leuven Chem&Tech for providing access to FTIR spectrophotometers.

ABBREVIATIONS

API, active pharmaceutical ingredient; PEG, polyethylene glycol; IMC, indomethacin; T_g, glass transition temperatures; T_m, melting point; m-DSC, modulated differential scanning calorimetry; XRD, X-ray diffraction; FTIR, Fourier transform infrared; NMR, nuclear magnetic resonance; PLM, polarized light microscopy; CP/MAS, cross-polarization/magic angle spinning.

REFERENCES

1. Williams, H. D.; Trevaskis, N. L.; Charman, S. A.; Shanker, R. M.; Charman, W. N.; Pouton, C. W.; Porter, C. J. H. Strategies to address low drug solubility in discovery and development. *Pharmacol. Rev.* **2013,** *65,* (1), 315-499.

2. Leuner, C.; Dressman, J. Improving drug solubility for oral delivery using solid dispersions. *Eur. J. Pharm. Biopharm.* **2000,** *50*, (1), 47-60.

3. Van den Mooter, G. The use of amorphous solid dispersions: A formulation strategy to overcome poor solubility and dissolution rate. *Drug Discov. Today Technol.* **2012,** *9*, (2), e79-e85.

4. Van Duong, T.; Van den Mooter, G. The role of the carrier in the formulation of pharmaceutical solid dispersions. Part I: crystalline and semi-crystalline carriers. *Expert Opin. Drug Deliv.* **2016,** *13*, (11), 1583-1594.

5. Van Duong, T.; Van den Mooter, G. The role of the carrier in the formulation of pharmaceutical solid dispersions. Part II: amorphous carriers. *Expert Opin. Drug Deliv.* **2016**, (just-accepted).

6. Granick, S.; Kumar, S. K.; Amis, E. J.; Antonietti, M.; Balazs, A. C.; Chakraborty, A. K.; Grest, G. S.; Hawker, C.; Janmey, P.; Kramer, E. J. Macromolecules at surfaces: Research challenges and opportunities from tribology to biology. *J. Polym. Sci., Part B: Polym. Phys.* **2003,** *41*, (22), 2755-2793.

7. Ilevbare, G. A.; Liu, H.; Edgar, K. J.; Taylor, L. S. Inhibition of solution crystal growth of ritonavir by cellulose polymers–factors influencing polymer effectiveness. *CrystEngComm* **2012,** *14*, (20), 6503-6514.

8. Schram, C. J.; Beaudoin, S. P.; Taylor, L. S. Impact of polymer conformation on the crystal growth inhibition of a poorly water-soluble drug in aqueous solution. *Langmuir* **2014,** *31*, (1), 171-179.

9. Minko, S.; Kiriy, A.; Gorodyska, G.; Stamm, M. Single flexible hydrophobic polyelectrolyte molecules adsorbed on solid substrate: transition between a stretched chain, necklace-like conformation and a globule. *J. Am. Chem. Soc.* **2002,** *124*, (13), 3218-3219.

10. Ayenew, Z.; Paudel, A.; Van den Mooter, G. Can compression induce demixing in amorphous solid dispersions? A case study of naproxen–PVP K25. *Eur. J. Pharm. Biopharm.* **2012,** *81*, (1), 207-213.

11. Zhu, Q.; Taylor, L. S.; Harris, M. T. Evaluation of the microstructure of semicrystalline solid dispersions. *Mol. Pharmaceutics* **2010,** *7*, (4), 1291-1300.

12. Zhu, Q.; Harris, M. T.; Taylor, L. S. Modification of crystallization behavior in drug/polyethylene glycol solid dispersions. *Mol. Pharmaceutics* **2012,** *9*, (3), 546-553.

13. Duong, T. V.; Van Humbeeck, J.; Van den Mooter, G. Crystallization kinetics of indomethacin/polyethylene glycol dispersions containing high drug loadings. *Mol. Pharmaceutics* **2015,** *12*, (7), 2493-2504.

14. Dordunoo, S. K.; Ford, J. L.; Rubinstein, M. H. Solidification studies of polyethylene glycols, gelucire 44/14 or their dispersions with triamterene or temazepam. *J. Pharm. Pharmacol.* **1996,** *48*, (8), 782-789.

15. Ford, J. L.; Stewart, A. F.; Dubois, J.-L. The properties of solid dispersions of indomethacin or phenylbutazone in polyethylene glycol. *Int. J. Pharm.* **1986,** *28*, (1), 11-22.

16. Fini, A.; Rodriguez, L.; Cavallari, C.; Albertini, B.; Passerini, N. Ultrasound-compacted and spray-congealed indomethacin/polyethyleneglycol systems. *Int. J. Pharm.* **2002,** *247*, (1), 11-22.

17. Valizadeh, H.; Nokhodchi, A.; Qarakhani, N.; Zakeri-Milani, P.; Azarmi, S.; Hassanzadeh, D.; Löbenberg, R. Physicochemical characterization of solid dispersions of indomethacin with PEG 6000, Myrj 52, lactose, sorbitol, dextrin, and Eudragit® E100. *Drug Dev. Ind. Pharm.* **2004,** *30*, (3), 303-317.

18. Kaneniwa, N.; Otsuka, M.; Hayashi, T. Physicochemical characterization of indomethacin polymorphs and the transformation kinetics in ethanol. *Chem. Pharm. Bull.* **1985,** *33*, (8), 3447-3455.

19. Margarit, M. V.; Rodríguez, I. C.; Cerezo, A. Physical characteristics and dissolution kinetics of solid dispersions of ketoprofen and polyethylene glycol 6000. *Int. J. Pharm.* **1994,** *108*, (2), 101-107.

20. Schachter, D. M.; Xiong, J.; Tirol, G. C. Solid state NMR perspective of drug–polymer solid solutions: a model system based on poly (ethylene oxide). *Int. J. Pharm.* **2004,** *281*, (1), 89-101.

21. Ozeki, T.; Yuasa, H.; Kanaya, Y. Application of the solid dispersion method to the controlled release of medicine. IX. Difference in the release of flurbiprofen from solid dispersions with poly (ethylene oxide) and hydroxypropylcellulose and the interaction between medicine and polymers. *Int. J. Pharm.* **1997,** *155*, (2), 209-217.

22. Lacoulonche, F.; Chauvet, A.; Masse, J. An investigation of flurbiprofen polymorphism by thermoanalytical and spectroscopic methods and a study of its interactions with poly-(ethylene glycol) 6000 by differential scanning calorimetry and modelling. *Int. J. Pharm.* **1997,** *153*, (2), 167-179.

23. Lacoulonche, F.; Chauvet, A.; Masse, J.; Egea, M.; Garcia, M. An investigation of FB interactions with poly (ethylene glycol) 6000, poly (ethylene glycol) 4000, and poly-ϵ-caprolactone by thermoanalytical and spectroscopic methods and modeling. *J. Pharm. Sci.* **1998,** *87*, (5), 543-551.

24. Borka, L. The polymorphism of indomethacine. New modifications, their melting behavior and solubility. *Acta Pharm. Suec.* **1974,** *11*, (3), 295.

25. Lin, S. Y. Isolation and solid-state characteristics of a new crystal form of indomethacin. *J. Pharm. Sci.* **1992,** *81*, (6), 572-576.

26. Surwase, S. A.; Boetker, J. P.; Saville, D.; Boyd, B. J.; Gordon, K. C.; Peltonen, L.; Strachan, C. J. Indomethacin: New polymorphs of an old drug. *Mol. Pharmaceutics* **2013,** *10*, (12), 4472-4480.

27. Kistenmacher, T. J.; Marsh, R. E. Crystal and molecular structure of an antiinflammatory agent, indomethacin, 1-(p-chlorobenzoyl)-5-methoxy-2-methylindole-3-acetic acid. *J. Am. Chem. Soc.* **1972,** *94*, (4), 1340-1345.

28. Chen, X.; Morris, K. R.; Griesser, U. J.; Byrn, S. R.; Stowell, J. G. Reactivity differences of indomethacin solid forms with ammonia gas. *J. Am. Chem. Soc.* **2002,** *124*, (50), 15012-15019.

29. Taylor, L. S.; Zografi, G. Spectroscopic characterization of interactions between PVP and indomethacin in amorphous molecular dispersions. *Pharm. Res.* **1997,** *14*, (12), 1691-1698.

30. Yuan, X.; Xiang, T.-X.; Anderson, B. D.; Munson, E. J. Hydrogen bonding interactions in amorphous indomethacin and its amorphous solid dispersions with poly (vinylpyrrolidone) and poly (vinylpyrrolidone-co-vinyl acetate) studied using 13C solid-state NMR. *Mol. Pharmaceutics* **2015,** *12*, (12), 4518-4528.

31. Paudel, A.; Geppi, M.; Van den Mooter, G. Structural and dynamic properties of amorphous solid dispersions: The role of solid-state nuclear magnetic resonance spectroscopy and relaxometry. *J. Pharm. Sci.* **2014,** *103*, (9), 2635-2662.

32. Adriaensens, P.; Storme, L.; Carleer, R.; Gelan, J.; Du Prez, F. Comparative morphological study of poly (dioxolane)/poly (methyl methacrylate) segmented networks and blends by 13C solid-state NMR and thermal analysis. *Macromolecules* **2002,** *35*, (10), 3965-3970.

33. Lequieu, W.; Van De Velde, P.; Du Prez, F. E.; Adriaensens, P.; Storme, L.; Gelan, J. Solid state NMR study of segmented polymer networks: fine-tuning of phase morphology via their molecular design. *Polymer* **2004,** *45*, (23), 7943-7951.

34. Chambon, S.; Mens, R.; Vandewal, K.; Clodic, E.; Scharber, M.; Lutsen, L.; Gelan, J.; Manca, J.; Vanderzande, D.; Adriaensens, P. Influence of octanedithiol on the nanomorphology

of PCPDTBT: PCBM blends studied by solid-state NMR. *Sol. Energ. Mat. Sol. Cells* **2012,** *96*, 210-217.

35. Apperley, D. C.; Forster, A. H.; Fournier, R.; Harris, R. K.; Hodgkinson, P.; Lancaster, R. W.; Rades, T. Characterisation of indomethacin and nifedipine using variable-temperature solid-state NMR. *Magn. Reson. Chem.* **2005,** *43*, (11), 881-892.

36. Masuda, K.; Tabata, S.; Kono, H.; Sakata, Y.; Hayase, T.; Yonemochi, E.; Terada, K. Solid-state ^{13}C NMR study of indomethacin polymorphism. *Int. J. Pharm.* **2006,** *318*, (1), 146-153.

37. Chu, P.; Wu, H.-D. Solid state NMR studies of hydrogen bonding network formation of novolac type phenolic resin and poly (ethylene oxide) blend. *Polymer* **2000,** *41*, (1), 101-109.

38. Pielichowska, K.; Głowinkowski, S.; Lekki, J.; Biniaś, D.; Pielichowski, K.; Jenczyk, J. PEO/fatty acid blends for thermal energy storage materials. Structural/morphological features and hydrogen interactions. *Eur. Polym. J.* **2008,** *44*, (10), 3344-3360.

39. Leiserowitz, L.; Schmidt, G. Molecular packing modes. Part III. Primary amides. *J. Chem. Soc. A* **1969**, 2372-2382.

40. Etter, M. C. Encoding and decoding hydrogen-bond patterns of organic compounds. *Acc. Chem. Res.* **1990,** *23*, (4), 120-126.

41. Gardiner, D. J.; Lees, A. J.; Straughan, B. P. A study of intermolecular hydrogen bonding in formamide by vibrational spectroscopy. *J. Mol. Struct.* **1979,** *53*, 15-24.

42. Heinz, A.; Gordon, K. C.; McGoverin, C. M.; Rades, T.; Strachan, C. J. Understanding the solid-state forms of fenofibrate–a spectroscopic and computational study. *Eur. J. Pharm. Biopharm.* **2009,** *71*, (1), 100-108.

43. Leiserowitz, L. Molecular packing modes. Carboxylic acids. *Acta Crystallogr. B Struct. Crystallo. Cryst. Chem.* **1976,** *32*, (3), 775-802.

44. Lifson, S.; Hagler, A.; Dauber, P. Consistent force field studies of intermolecular forces in hydrogen-bonded crystals. 1. Carboxylic acids, amides, and the C=O•••H-hydrogen bonds. *J. Am. Chem. Soc.* **1979,** *101*, (18), 5111-5121.

45. Spegt, P. P. Rôle de la masse moléculaire sur la structure lamellaire des polyoxyéthylenes. *Die Makromolekulare Chemie* **1970,** *140*, (1), 167-177.

46. Godovsky, Y. K.; Slonimsky, G.; Garbar, N. Effect of molecular weight on the crystallization and morphology of poly (ethylene oxide) fractions. *J. Polym. Sci., Part C: Polym. Symp.* **1972,** *38*, 1-21.

47. Maclaine, J.; Booth, C. Effect of molecular weight on spherulite growth rates of high molecular weight poly (ethylene oxide) fractions. *Polymer* **1975,** *16*, (3), 191-195.

48. Janssens, S.; Denivelle, S.; Rombaut, P.; Van den Mooter, G. Influence of polyethylene glycol chain length on compatibility and release characteristics of ternary solid dispersions of itraconazole in polyethylene glycol/hydroxypropylmethylcellulose 2910 E5 blends. *Eur. J. Pharm. Sci*. **2008,** *35*, (3), 203-210.

49. Baird, J. A.; Van Eerdenbrugh, B.; Taylor, L. S. A classification system to assess the crystallization tendency of organic molecules from undercooled melts. *J. Pharm. Sci.* **2010,** *99*, (9), 3787-3806.

50. Tadokoro, H.; Chatani, Y.; Yoshihara, T.; Tahara, S.; Murahashi, S. Structural studies on polyethers,$[-(CH2)_m-O-]_n$. II. Molecular structure of polyethylene oxide. *Die makromolekulare chemie* **1964,** *73*, (1), 109-127.

51. Koenig, J.; Angood, A. Raman spectra of poly(ethylene glycols) in solution. *J. Polym. Sci., Part A-2: Polym. Phys.* **1970,** *8*, (10), 1787-1796.

52. Kovacs, A.; Gonthier, A.; Straupe, C. Isothermal growth, thickening, and melting of poly (ethylene oxide) single crystals in the bulk. *J. Polym.Sci.: Polym. Symp.* **1975,** *50*, 283-325.

53. Hoffman, J. D.; Miller, R. L. Kinetic of crystallization from the melt and chain folding in polyethylene fractions revisited: theory and experiment. *Polymer* **1997,** *38*, (13), 3151-3212.

54. Yamamoto, T. Molecular dynamics simulation of polymer crystallization through chain folding. *J. Chem. Phys.* **1997,** *107*, (7), 2653-2663.

55. Yang, M.; Gogos, C. Crystallization of poly (ethylene oxide) with acetaminophen–A study on solubility, spherulitic growth, and morphology. *Eur. J. Pharm. Biopharm.* **2013,** *85*, (3), 889-897.

56. Matsumoto, T.; Zografi, G. Physical properties of solid molecular dispersions of indomethacin with poly (vinylpyrrolidone) and poly (vinylpyrrolidone-co-vinyl-acetate) in relation to indomethacin crystallization. *Pharm. Res.* **1999,** *16*, (11), 1722-1728.

57. Russell, T.; Ito, H.; Wignall, G. Neutron and X-ray scattering studies on semicrystalline polymer blends. *Macromolecules* **1988,** *21*, (6), 1703-1709.

58. Dubois, J. L.; Ford, J. L. Similarities in the release rates of different drugs from polyethylene glycol 6000 solid dispersions. *J. Pharm. Pharmacol.* **1985,** *37*, (7), 494-495.

59. Dordunoo, S.; Ford, J.; Rubinstein, M. Preformulation studies on solid dispersions containing triamterene or temazepam in polyethylene glycols or Gelucire 44/14 for liquid filling of hard gelatin capsules. *Drug Dev. Ind. Pharm.* **1991,** *17*, (12), 1685-1713.

60. Vippagunta, S. R.; Wang, Z.; Hornung, S.; Krill, S. L. Factors affecting the formation of eutectic solid dispersions and their dissolution behavior. *J. Pharm. Sci.* **2007,** *96*, (2), 294-304.

61. Yeh, F.; Hsiao, B. S.; Chu, B.; Sauer, B. B.; Flexman, E. A. Effect of miscible polymer diluents on the development of lamellar morphology in poly (oxymethylene) blends. *J. Polym. Sci., Part B: Polym. Phys.* **1999,** *37*, (21), 3115-3122.

62. Dreezen, G.; Ivanov, D.; Nysten, B.; Groeninckx, G. Nano-structured polymer blends: phase structure, crystallisation behaviour and semi-crystalline morphology of phase separated

binary blends of poly (ethylene oxide) and poly (ether sulphone). *Polymer* **2000,** *41*, (4), 1395-1407.